Mathematisches Forschungsinstitut Oberwolfach

Report No. 02/2009

DOI: 10.4171/OWR/2009/02

Discrete Differential Geometry

Organised by
Alexander I. Bobenko, Berlin
Richard Kenyon, Providence, RI
John Sullivan, Berlin
Günter M. Ziegler, Berlin

January 11th – January 17th, 2009

Abstract. This is the collection of extended abstracts for the 26 lectures and the open problems session at the second Oberwolfach workshop on Discrete Differential Geometry.

Mathematics Subject Classification (2000): 52-xx, 53-xx, 57-xx.

Introduction by the Organisers

Discrete Differential Geometry is an active mathematical terrain where differential geometry (the theory of smooth manifolds, providing notions of curvature, flows, integrability, etc.) interacts with discrete geometry (concerned with polyhedral surfaces, frameworks and their rigidity, polytopes and their subdivisions, etc.), using tools and ideas from all parts of mathematics, including, for example, conformal geometry, integrable systems, algebraic combinatorics, mathematical physics (discrete electrodynamics, hydrodynamics and elasticity), computational geometry, and geometry processing.

In view of two books entitled "Discrete Differential Geometry" – the proceedings of the 2004 Oberwolfach Seminar (Birkhäuser 2008) and the recent volume by Bobenko & Suris (AMS 2008) – as well as a number of workshops in recent years (St. Petersburg 2003, Oberwolfach 2006, Berlin 2007) treating the subject, it can be said that Discrete Differential Geometry has started to be a well-established mathematical discipline. Nevertheless, the boundaries of the field are not fixed;

quite to the contrary, it is branching out into new directions, and new and sometimes unexpected connections and lines of development appear frequently – as can also be seen in the following pages.

The present collection of extended abstracts documents the lectures and the open problems session at the second Oberwolfach workshop on Discrete Differential Geometry. It records a successful and very active workshop, and thus presents a multi-facetted picture of the field. We are grateful to all the participants of the Workshop for their manifold contributions, and to the institute in Oberwolfach and all its staff for providing, once again, a perfect setting for this.

Workshop: Discrete Differential Geometry

Table of Contents

Abstracts

Semidiscrete Surface Representations

Johannes Wallner
(joint work with Christian Müller and Helmut Pottmann)

A semidiscrete surface representation $x(u,k)$ is a mapping $x : \mathbb{R} \times \mathbb{Z} \to \mathbb{R}^3$, i.e., a bivariate function with one continuous and one discrete parameter. It can be interpreted as the limit of discrete surfaces $(\varepsilon\mathbb{Z}) \times \mathbb{Z} \to \mathbb{R}^3$ as ε tends to zero. There is actually an entire spectrum of mappings $\mathbb{Z}^r \times \mathbb{R}^s \to \mathbb{R}^d$ of which the purely discrete and the purely continuous surfaces are the extremal cases, and which are discussed in depth by [2]. A major point of that theory is that for $r \geq 1$, $s \geq 2$ they represent the classical topic of transformations of surfaces, and that the limit viewpoint allows us to consider transformations and especially their permutability theorems within the theory of discrete integrable systems.

The low-dimensional case $r = d = 1$ turned out to be very interesting in its own right when in [4] the approximation of surfaces by a sequence of single-curved strips was discussed from the viewpoint of geometry processing, motivated by applications in architectural design. Such 'developable strip models' are recognized as semidiscrete conjugate nets, and their theory and specializations to circular and conical nets are developed by [4]. A general discussion of relations between discrete differential geometry and architectural design is given by [5].

In the following we report on results of [4] concerning conjugate nets, as well as material not yet published [3, 7].

Our basic entity is a *net* which can be discrete, semidiscrete, or continuous, and which is a mapping "x" defined in $\mathbb{Z} \times \mathbb{Z}$, or $\mathbb{R} \times \mathbb{Z}$, or $\mathbb{R} \times \mathbb{R}$, having values in $\mathbb{R}^3$. We write $x(j,k)$, $x(u,k)$, and $x(u,v)$, respectively. The dependence on the continuous parameters is understood to be C^2. We write $\partial_u x$ for derivatives w.r.t. smooth variables, and $\Delta_k x$ for discrete derivatives, i.e., forward differences.

Conjugate nets. These are defined by planarity of elementary (infinitesimal) quadrilaterals, which is expressed as the linear dependence of three vectors, namely

$$\Delta_j\Delta_k x,\ \Delta_j x,\ \Delta_k x, \quad \text{or} \quad \Delta_k\partial_u x,\ \Delta_k x,\ \partial_u x, \quad \text{or} \quad \partial_u\partial_v x,\ \partial_u x,\ \partial_v x,$$

in the three respective categories. For semidiscrete x this means that the *ruled strip* generated by curves $x|_{\mathbb{R}\times\{k\}}$ and $x|_{\mathbb{R}\times\{k+1\}}$, viz.,

$$s^{(k)} : \mathbb{R} \times [0,1] \to \mathbb{R}^3, \quad (u,v) \mapsto (1-v)x(u,k) + v\,x(u,k+1),$$

is *developable*. Circularity of the net means that each strip has a family of inscribed circles which are tangent to the boundary curves in corresponding points. In this way a developable strip is a 1D *Jonas transform*, which becomes a *Darboux transform* if the strip is in addition circular. The net is conical, if for each vertex there is a right circular cone tangent to the two adjacent strips. It turns out that circular and conical strips are convertible into each other and possess a nice focal theory similar to [6].

We have further investigated the circular nets with regard to equivalence, isothermicity, the Koenigs property, and Christoffel duality. It is instructive to demonstrate how properties like the incidence-geometric characterization of discrete Koenigs nets manifest themselves in the semidiscrete category. First the discrete version: *A discrete conjugate net is Koenigs* $\iff$ *The diagonals of elementary quadrilaterals intersect in the vertices of yet another conjugate net.* For the semidiscrete case it is first necessary to consider the limit of a planar 4-gon $abcd$ with points $e = ac \cap bd$, $f = bc \cap ad$ as shown, as $a \to b$ and $c \to d$:

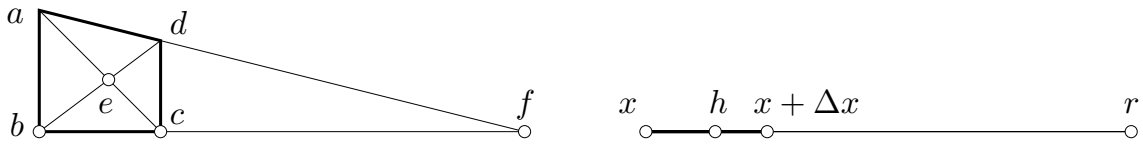

It is not difficult to see that the limit points have cross ratio -1, and that the interpretation of $abcd$ as an infinitesimal quad in a net yields the following: *A semidiscrete conjugate net x is Koenigs* $\iff$ *The net h which is defined by the condition that* $\mathrm{cr}(x, h, x + \Delta x, r) = -1$ *is itself a conjugate net*, where $r(u, k)$ is the singular point of the strip $s^{(k)}$ located on the ruling $x(u, k)x(u, k + 1)$.

Asymptotic nets. Also here there is much analogy between the three categories. Asymptotic nets (A-nets) are defined by the condition that the second derivatives w.r.t. both parameters are co-planar with the first derivatives. In the semidiscrete case this amounts to the condition that

$$\partial x,\ \partial^2 x,\ \Delta x,\ \Delta^- x$$

are co-planar, where Δ^- is the backwards difference, and where we dropped the indices after ∂, Δ. Consequently the union of ruled surface strips $\{s^{(k)}(\mathbb{R} \times [0, 1])\}_{k \in \mathbb{Z}}$ associated with an A-net is a *smooth* surface, provided it does not overfold, with the strip boundaries being asymptotic curves of each adjacent strip.

Each semidiscrete A-net (possibly after changing handedness) has a semidiscrete Lelieuvre vector field U with $\Delta x = U \times \Delta U$ and $\partial x = -U \times \partial U$ which is unique (like for continuous A-nets) and which fulfills a Moutard equation. In addition, the net $\widetilde{U}(u, k) = (-1)^k U(u, k)$ is a conjugate net (like in the discrete case): The ruled surface defined by the curves

$$-U|_{\mathbb{R} \times \{k\}}, \quad U|_{\mathbb{R} \times \{k+1\}},$$

is developable, with its curve of regression exactly in between at $\Delta U(u, k)/2$. This means that $\widetilde{U}$ is actually a *T-net*. Taking the definition

$$K = -\|U\|^{-4}$$

of Gauss curvature from the continuous category, we can show that A-nets of constant Gaussian curvature are characterized by the weak Chebyshev property:

$$K = \text{const.} \iff \Delta \|\partial x\| = \partial \|\Delta x\| = 0.$$

Further, both associated nets U, $\widetilde{U}$ enjoy the weak Chebyshev property. Knowing the relations between discrete and continuous A-nets of constant Gaussian curvature [1, 8], this theorem is to be expected. It is however interesting to observe the role of the T-net $\widetilde{U}$ in the proof of this fact.

This research is supported by the National Research Network *Industrial Geometry* (grant No. S92, Austrian Science Fund).

References

[1] A. Bobenko and U. Pinkall, *Discrete Surfaces with constant negative Gaussian curvature and the Hirota equation*, J. Differential Geom. **43** (1996), 527–611.
[2] A. Bobenko and Yu. Suris, *Discrete differential geometry: Integrable structure*, Graduate Studies in Math., vol. 98, American Math. Soc., 2008.
[3] C. Müller, *Semi-discrete isothermic surfaces*, forthcoming paper, 2009.
[4] H. Pottmann, A. Schiftner, P. Bo, H. Schmiedhofer, W. Wang, N. Baldassini, and J. Wallner. *Freeform surfaces from single curved panels.*, ACM Trans. Graphics **27** (2008), 76:1–76:10. [Proceedings of ACM SIGGRAPH '08]
[5] H. Pottmann, A. Schiftner, and J. Wallner, *Geometry of architectural freeform structures*, Int. Math. Nachr. **209** (2008), 15–28.
[6] H. Pottmann and J. Wallner, *The focal geometry of circular and conical meshes*, Adv. Comput. Math. **29** (2008), 249–268.
[7] J. Wallner, *Semidiscrete A-surfaces and K-surfaces*, forthcoming paper, 2009.
[8] W. Wunderlich, *Zur Differenzengeometrie der Flächen konstanter negativer Krümmung*, Österreich. Akad. Wiss. Math.-Nat. Kl. S.-B. IIa. **160** (1951), 39–77.

Discrete Differential Geometry: Integrable structure

Yuri B. Suris
(joint work with Alexander I. Bobenko)

This talk was based on the textbook with A. Bobenko [1] recently published by the AMS, and aimed at giving an overview of an (integrable part of) discrete differential geometry. *Discrete differential geometry* (DDG) develops discrete analogues and equivalents of notions and methods of differential geometry of smooth curves, surfaces etc. The smooth theory appears in a limit of the refinement of discretizations. *Integrable differential geometry* deals with parametrized objects (surfaces and coordinate systems) described by integrable differential equations. As integrability attributes one counts traditionally: zero curvature representations, transformations with remarkable permutability properties, hierarchies of commuting flows etc. Development of DDG led, somewhat unexpectedly, among other things, to a better understanding of the very notion of integrability.

The basic notion of DDG is that of a *discrete net*, i.e., a map $f : \mathbb{Z}^m \to \mathcal{X}$. Here $\mathcal{X}$ is some space; in the most straightforward examples, like Q-nets (or discrete conjugate nets), $\mathcal{X}$ is just the ambient space of the underlying geometry, like $\mathcal{X} = \mathbb{RP}^N$, however more intricate mathematical models require for other spaces $\mathcal{X}$, and a good deal of this talk was devoted to these less trivial situations. Notation for discrete nets: $f = f(u)$, $f_i = f(u + e_i)$, $f_{ij} = f(u + e_i + e_j)$, etc.

We started with the following definitions:

– A (hyperbolic) 2d system (with fields assigned to vertices) is a geometric condition, equation, etc., which allows to determine the 4th point of an elementary square of $\mathbb{Z}^2$ if other three are arbitrarily prescribed.
– A (hyperbolic) 3d system (with fields assigned to vertices) is a geometric condition, equation, etc., which allows to determine the 8th point of an elementary cube of $\mathbb{Z}^3$ if other seven are arbitrarily prescribed.

These notions are schematically represented in Figure 1. Natural boundary value problems for these systems are *Goursat problems* (prescribing initial data along coordinate axes for a 2d system, resp. along coordinate planes for a 3d system) and *Cauchy problems* (prescribing initial data along a non-characteristic staircase line, resp. along a non-characteristic stepped surface).

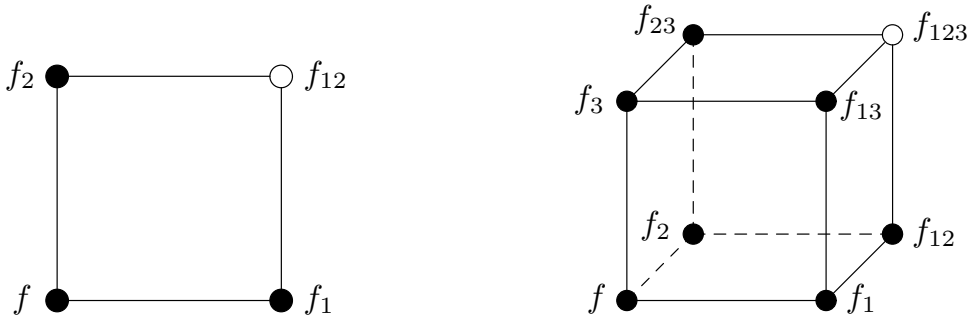

FIGURE 1. Elementary square of a 2d system (left) and an elementary cube of a 3d system (right). Black circles mark the initial data; white circles mark the vertices uniquely determined by the initial data.

One of the fundamental *organizing principles* of integrable DDG is the *multidimensional consistency principle*: discretizations of surfaces, coordinate systems and other parametrized objects should be extendable to multidimensionally consistent nets. Multidimensional consistency is, in our understanding, synonymous with integrability. For a 2d system, it is enough to establish its 3d consistency, and likewise for a 3d system it is enough to establish its 4d consistency. These notions are schematically represented in Figure 2. Given a multidimensionally consistent discrete net, a smooth limit in some of the coordinate directions leads to smooth surfaces with transformations possessing permutability properties. As a rule, consistency is a consequence of elementary incidence theorems of geometry, which therefore constitute a true root of integrable differential geometry.

Several classes of discrete nets were considered, with an emphasis on the situations where a less simple choice of the space $\mathcal{X}$ becomes crucial.

• The most fundamental class of discrete nets constitute Q-nets $f : \mathbb{Z}^m \to \mathbb{RP}^N$, characterized by the property that four vertices of each elementary quadrilateral lie in a plane. A generalization has been recently proposed in [2]: *Grassmannian Q-nets* are nets $f : \mathbb{Z}^m \to \mathbb{G}_r^N$ with values in the Grassmannian $\mathbb{G}_r^N$ of r-planes in $\mathbb{RP}^N$, characterized by the property that for each elementary quadrilateral the four r-planes f, f_i, f_j and f_{ij} assigned to its vertices span a $(3r+2)$-plane. (Usual

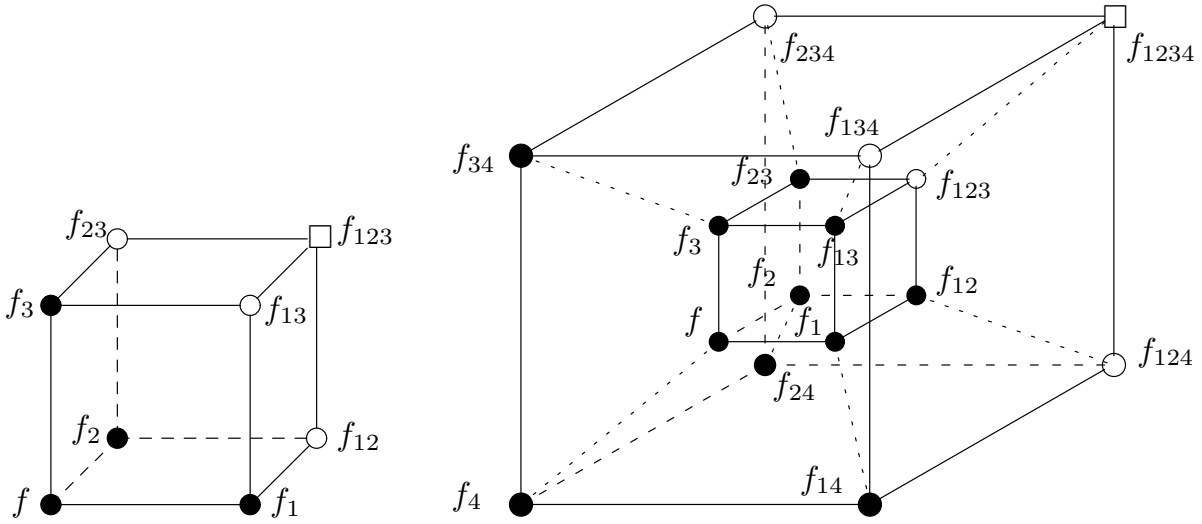

FIGURE 2. 3d consistency of a 2d system (left) and 4d consistency of a 3d system (right). Black circles mark the initial data; white circles mark the vertices uniquely determined by the initial data; white square marks the vertex where the consistency condition appears.

Q-nets correspond to $r = 0$.) It has been proven in [2] that Grassmannian Q-nets, like the usual ones, are described by a multidimensionally consistent 3d system.

• Another remarkable class of discrete nets described by a 3d system featuring multidimensional consistency constitute *A-nets* $f : \mathbb{Z}^m \to \mathbb{RP}^3$, characterized by the property that all neighbor points $f(u \pm e_i)$ of $f(u)$ lie in a plane $\mathcal{P}(u)$ through $f(u)$. It turns out to be natural to consider A-nets as maps with values in the space $\mathcal{X}$ of all pairs $(f, \mathcal{P})$ satisfying $f \in \mathcal{P}$, characterized by the condition that for two neighboring pairs $(f, \mathcal{P}) \sim (f_i, \mathcal{P}_i)$ there holds $f \in \mathcal{P}_i$ and $f_i \in \mathcal{P}$. The incidence theorem underlying the 4d consistency of this system is that of MÖBIUS on the pairs of mutually inscribed tetrahedra. The space $\mathcal{X}$ of contact elements admits a beautiful realization in the framework of Plücker line geometry: contact elements $(f, \mathcal{P})$ are interpreted as sets of lines in $\mathcal{P}$ through f and are represented by isotropic lines in the Plücker quadric in $\mathbb{P}(\mathbb{R}^{3,3})$. The characteristic property of A-nets reduces to the condition that any two neighboring isotropic lines ℓ, ℓ_i intersect. In other words, A-nets correspond to discrete congruences of isotropic lines in the Plücker quadric.

• If one interprets contact elements $(f, \mathcal{P})$ in the framework of Lie sphere geometry as the sets of all spheres through f in oriented contact with $\mathcal{P}$, one arrives at the notion of *principal contact element nets*, which serve as a discretization of the curvature line parametrized surfaces. The defining condition is that for two neighboring pairs $(f, \mathcal{P}) \sim (f_i, \mathcal{P}_i)$ there is a sphere through both f and f_i in oriented contact with both $\mathcal{P}$ and $\mathcal{P}_i$. The points of a principal contact element net build a circular net, while the planes build a conical net. In the framework of Lie sphere geometry, the space $\mathcal{X}$ of contact elements admits a realization as the

space of isotropic lines in the Lie quadric in $\mathbb{P}(\mathbb{R}^{4,2})$. The characteristic property of principal contact element nets translates to the condition that any two neighboring isotropic lines ℓ, ℓ_i intersect. Thus, principal contact element nets correspond to discrete congruences of isotropic lines in the Lie quadric.

In conclusion, it has been stressed that multidimensional consistency serves as the organizing principle of integrable discrete differential geometry, and that interesting geometries appear as discrete nets in some less trivial spaces $\mathcal{X}$. Presumably, many important examples still wait to be discovered.

References

[1] A. I. Bobenko, Yu. B. Suris, *Discrete Differential Geometry: Integrable Structure*. Graduate Studies in Mathematics, Vol. 98. AMS, 2008. xxiv+404 pp.

[2] V. E. Adler, A. I. Bobenko, Yu. B. Suris. Integrable discrete nets in Grassmannians. arXiv: 0812.5102 [math.DG].

Discrete Ricci curvature for metric spaces and Markov chains

Yann Ollivier

We define the coarse Ricci curvature of metric spaces in terms of how much small balls are closer (in Wasserstein transportation distance) than their centers are. This definition naturally extends to any Markov chain on a metric space. For a Riemannian manifold this gives back, after scaling, the value of Ricci curvature of a tangent vector. Examples of positively curved spaces for this definition include graphs such as the discrete cube. Moreover this generalization is consistent with the Bakry–Émery Ricci curvature for Brownian motion with a drift on a Riemannian manifold.

Positive Ricci curvature implies a spectral gap, a Lévy–Gromov–like Gaussian concentration theorem and a kind of modified logarithmic Sobolev inequality. The bounds obtained are sharp in a variety of examples.

Our starting point is the following: Is there a common geometric feature between the N-dimensional sphere S^N, the discrete cube $\{0,1\}^N$, and the space $\mathbb{R}^N$ equipped with a Gaussian measure? For a start, all three spaces exhibit the *concentration of measure* phenomenon [Led01]; moreover, by the Dvoretzky theorem random small-dimensional sections of the cube are close to a sphere, and small-dimensional projections of either the sphere or the cube give rise to nearly-Gaussian measures.

So one can wonder whether there exists a common underlying geometric property. A hint is given by the Gromov–Lévy theorem [Gro86], which states that Gaussian concentration occurs not only for the N-dimensional sphere, but for all Riemannian manifolds of *positive curvature* in the sense that their *Ricci curvature* is at least that of the sphere. In Riemannian geometry, Ricci curvature is the relevant notion in a series of positive-curvature theorems.

One is left with the problem of finding a definition of Ricci curvature valid for spaces more general than Riemannian manifolds. Moreover, the definition should

be local and not global, since the idea of curvature is to seek local properties entailing global constraints. A first step in this direction is provided by Bakry–Émery theory [BE85], which allows to define the Ricci curvature of a diffusion process on a Riemannian manifold (or equivalently, of a second-order differential operator); when the diffusion is ordinary Brownian motion, this gives back usual Ricci curvature. When applied to the natural process on $\mathbb{R}^N$ associated with the Gaussian measure, this yields a positive curvature for the Gaussian space.

Because the Bakry–Émery definition involves differential calculus, it is not readily adaptable to discrete spaces. If one wants to deal with the third basic example, the discrete cube, one has to drop the continuity aspect and deal with more "robust" or "coarse" notions that forget the small-scale properties of the underlying space. This is similar in spirit to what has been done for a long time in the (very different) world of *negative curvature*, for which coarse notions such as δ-hyperbolicity and CAT(0) spaces have been developed.

Such a notion can be summarized as follows [Oll07, Oll09]: a metric space has positive curvature if *small balls are closer than their centers are*. Here one uses *transportation distances* [Vil03] to measure the distance between balls.

It is possible to put emphasis on a random process (consistently with Bakry–Émery theory) and replace the ball centered at a point with the transition probability of a random walk. Doing so, one finds that the property above is equivalent to a property first introduced by Dobrushin [Dob70, DS85] for Markov fields, and still known in the Ising community as the "Dobrushin criterion" (several variants of which are in use). The 1970 Dobrushin paper was actually the one to make transportation distances known to a wider audience.

Examples. Here are some spaces for which coarse Ricci curvature can be easily computed:
- Riemannian manifolds: we get usual Ricci curvature up to some scaling.
- The discrete cube $\{0,1\}^N$: coarse Ricci curvature is positive.
- $\mathbb{Z}^n$ with its lattice metric: coarse Ricci curvature is 0.
- Diffusions on a manifold: we recover the Bakry–Émery curvature, in a more visual way.
- Multinomial distributions, waiting queues, and similar examples.
- Ising model and its variants: coarse Ricci curvature depends on temperature, in an explicit way.
- δ-hyperbolic groups: coarse Ricci curvature is negative.

Results. Here are some of the results obtained when coarse Ricci curvature is positive:
- Concentration results (Gaussian or exponential concentration) as in the Gromov–Lévy theorem.
- Spectral gap estimate as in the Lichnerowicz theorem.
- Logarithmic Sobolev inequality and gradient contraction by the heat kernel, as in Bakry–Émery theory.

– Convergence rates of the underlying Markov chain; in particular, explicit convergence rates for the Markov chain Monte Carlo (MCMC) method.
– Good behavior in Gromov–Hausdorff topology.

References

[BE85] D. Bakry, M. Émery, *Diffusions hypercontractives*, Séminaire de probabilités, XIX, 1983/84. Lecture Notes in Math. **1123**, Springer, Berlin (1985), 177–206.

[Dob70] R. L. Dobrušin, *Definition of a system of random variables by means of conditional distributions* (Russian), Teor. Verojatnost. i Primenen. **15** (1970), 469–497. English translation: *Prescribing a system of random variables by conditional expectations*, Theory of Probability and its Applications **15** (1970) nr. 3, 458–486.

[DS85] R. L. Dobrushin, S. B. Shlosman, *Constructive criterion for the uniqueness of Gibbs field*, in J. Fritz, A. Jaffe and D. Szász (eds), *Statistical physics and dynamical systems*, papers from the second colloquium and workshop on random fields: rigorous results in statistical mechanics, held in Köszeg, August 26–September 1, 1984, Progress in Physics **10**, Birkhäuser, Boston (1985), 347–370.

[Gro86] M. Gromov, *Isoperimetric inequalities in Riemannian manifolds*, in V. Milman, G. Schechtman, *Asymptotic theory of finite dimensional normed spaces*, Lecture Notes in Mathematics **1200**, Springer, Berlin (1986), 114–129.

[Led01] M. Ledoux, *The concentration of measure phenomenon*, Mathematical Surveys and Monographs **89**, AMS (2001).

[Oll07] Y. Ollivier, *Ricci curvature of metric spaces*, C. R. Math. Acad. Sci. Paris **345** (2007), nr. 11, 643–646.

[Oll09] Y. Ollivier, *Ricci curvature of Markov chains on metric spaces*, J. Funct. Anal. **256** (2009), nr. 3, 810–864.

[Vil03] C. Villani, *Topics in optimal transportation*, Graduate Studies in Mathematics **58**, American Mathematical Society, Providence (2003).

The discrete Hilbert-Einstein functional: History and applications

Ivan Izmestiev

1. The total mean curvature

Jacob Steiner found in 1840 that the volume of the parallel body

$$K_t = \{x \mid \operatorname{dist}(x, K) \leq t\}$$

to a convex body $K \subset \mathbb{R}^3$ can be expanded as

$$\operatorname{vol}(K_t) = \operatorname{vol}(K) + t \cdot \operatorname{area}(\partial K) + t^2 \cdot S(K) + t^3 \cdot \frac{4\pi}{3}, \tag{1}$$

provided that K is either a polytope or a body with smooth boundary. If K is a polytope, then the coefficient at t^2 is

$$S(K) = \frac{1}{2} \sum_e \ell_e(\pi - \theta_e), \tag{2}$$

where the sum is taken over all edges of K, and ℓ_e is the length of, θ_e is the dihedral angle at the edge e. If K is a body with smooth boundary, then we have

$$S(K) = \int_{\partial K} \frac{k_1 + k_2}{2}\, d\,\text{area}, \tag{3}$$

where k_1 and k_2 are the principal curvatures of the boundary of K. This is a reason to call the sum (2) *the total mean curvature* of the polyhedral surface ∂K.

Later, Steiner's argument war reinforced by Minkowski who proved that the expansion (1) holds for an arbitrary convex body K, and its coefficients depend continuously on K in the Hausdorff metric. In particular, if a convex body with smooth boundary is approximated by convex polytopes, then (2) converges to (3).

2. The total scalar curvature, or the Hilbert-Einstein functional

Let M be a closed manifold equipped with a Riemannian metric g. The *Hilbert-Einstein* functional is the integral of the scalar curvature

$$S(g) = \int_M s_g \, d\,\text{vol}_g\,. \tag{4}$$

Theorem 1 (Hilbert)**.** *For a fixed manifold M, consider the space of all unit volume metrics g. Then the critical points of S correspond to Einstein metrics.*

Unfortunately, the functional S is neither bounded from above, nor from below, so that critical points are hard to find. But there are good news too.

Theorem 2 (Yamabe, see [6])**.** *On the space of the unit volume metrics conformally equivalent to g*

$$\{u \cdot g \mid u : M \to \mathbb{R}_+,\, \text{vol}_{u\cdot g}(M) = 1\},$$

the functional S can be minimized. The point of minimum is a metric of constant scalar curvature.

The *discrete Hilbert-Einstein functional* for $\dim M = 3$ is defined as follows. Call a discrete Riemannian metric on M a pair (T, ℓ) of a triangulation T of M and an assignment $\ell : e \mapsto \ell_e$ of a positive number to every edge of T such that the tetrahedra of T can be realized as Euclidean ones with edge lengths ℓ_e. Let

$$S(T, \ell) = \sum_e \ell_e(2\pi - \omega_e), \tag{5}$$

where ω_e is the angle around e. The functional (5) is also known as the Regge functional, and can be defined with hyperbolic or spherical tetrahedra as well.

Similarly to Section 1, (5) converges to (4) (up to a constant factor), when the discrete Riemannian metric (T, ℓ) converges to the Riemannian metric g, see [3].

Theorem 3. *The discrete Hilbert-Einstein functional* (5) *has the property*

$$\frac{\partial S}{\partial \ell_e} = 2\pi - \omega_e =: \kappa_e \tag{6}$$

Thus, the critical points of S correspond to Euclidean metrics on M, subdivided by the triangulation T.

Equation (6) is a direct consequence of the Schläfli formula.

Consider the matrix of the second partial derivatives of S

$$\text{Hess}(S) = \left(\frac{\partial^2 S}{\partial \ell_i \partial \ell_j} \right) = \left(\frac{\partial \kappa_i}{\partial \ell_j} \right). \tag{7}$$

- If $\text{Hess}(S)$ is positive (negative) semidefinite, then S is convex (concave).
- If $\det \text{Hess}(S) \neq 0$, then the metric (T, ℓ) is infinitesimally rigid, that is a non-zero first-order change in ℓ entails a non-zero first-order change in κ.

3. Partial results on the signature of $\text{Hess}(S)$

A discrete Riemannian metric (T, ℓ) is called a *ball packing metric*, if there exists a function $r : i \mapsto r_i$ on the set of vertices of T such that $\ell_{ij} = r_i + r_j$ holds for all edges ij.

Theorem 4 (Cooper, Rivin [4]). *The functional S is convex on the space of all ball packing metrics. The nullspace of the Hessian is one-dimensional and corresponds to scaling.*

A consequence of Theorem 4 is the infinitesimal rigidity of ball packings in 3–dimensional manifolds.

A change of ℓ defined by $\ell'_{ij} = \ell_{ij} + u_i + u_j$ can be viewed as a discrete analog of a conformal deformation; then Theorem 4 says that S is convex on the conformal class of an "equilateral" metric $\{\ell_{ij} = 1 \text{ for all } ij\}$.

In the next two theorems the discrete Hilbert-Einstein functional of manifolds with boundary is considered. It is obtained by adding to (5) a boundary term similar to (2). We consider only deformations that preserve the metric on the boundary. The property (6) remains valid for deformations of the interior edges.

Theorem 5 (I., Schlenker [5]). *Let $M \approx \mathbb{B}^3$, and let the metric (T, ℓ) on $\mathbb{B}^3$ be such that $\omega_e = 2\pi$ for all interior edges and $\theta_e \leq \pi$ for all boundary edges. That is, let (T, ℓ) be a triangulation of a convex polytope P. Let*

i = the number of the interior vertices of T;

f = the number of the boundary vertices of T not in the 1–skeleton of P.

Then the Hessian (7) has corank $3i + f$ and exactly i positive eigenvalues.

In particular, the Hessian is negatively definite, if there are no interior vertices and no vertices inside the faces of P. This fact was used in [5] to prove the infinitesimal rigidity for a class of non-convex polytopes.

Note that the number of positive eigenvalues in Theorem 5 is equal to the dimension of the space of conformal deformations. However, we were unable to describe an i–dimensional space of deformations on which the Hessian would be positively definite.

Theorem 6 (Bobenko, I. [2]). *Let $M \approx \mathbb{B}^3$, let T be the cone over a triangulation of $\mathbb{S}^2$, and let $\theta_e \leq \pi$ for all boundary edges. The interior edges are then in one-to-one correspondence with the boundary vertices.*

- *Assume that $\phi_i < \omega_i < 2\pi$, where ϕ_i is the angle around the vertex i in the metric on $\mathbb{S}^2$. Then* $\mathrm{Hess}(S)$ *is non-degenerate and has at least one positive eigenvalue. Namely, $d\ell_i = \frac{1}{\ell_i}$ is a positive direction for* $\mathrm{Hess}(S)$.
- *Assume that $\omega_i = 2\pi$ for all i, so that (T, ℓ) is a triangulation of a convex polytope. Then* $\mathrm{Hess}(S)$ *has corank* 3 *and exactly one positive eigenvalue. The vectors $d\ell_i = \frac{1}{\ell_i}$ and $d\ell_i = 1$ both belong to its positive cone.*

The first statement of Theorem 6 suggests that $(\ell'_{ij})^2 = \ell_{ij}^2 + u_i + u_j$ could be considered as a discrete analog of a conformal deformation.

The main result of [2] is a new proof of Alexandrov's theorem on the existence of a convex polytope with a given metric on the boundary. Note that for its smooth analog, Weyl's problem, a variational approach based on the Hilbert-Einstein functional was proposed by Blaschke and Herglotz in [1].

References

[1] W. Blaschke and G. Herglotz. Über die Verwirklichung einer geschlossenen Fläche mit vorgeschriebenem Bogenelement im Euklidischen Raum. *Sitzungsber. Bayer. Akad. Wiss., Math.-Naturwiss. Abt.* 1937, 229–230 (No. 2) (1937).

[2] A. I. Bobenko and I. Izmestiev. Alexandrov's theorem, weighted Delaunay triangulations, and mixed volumes. *Ann. Inst. Fourier (Grenoble)*, 58(2):447–505, 2008.

[3] J. Cheeger, W. Müller, and R. Schrader. On the curvature of piecewise flat spaces. *Comm. Math. Phys.*, 92(3):405–454, 1984.

[4] D. Cooper and I. Rivin. Combinatorial scalar curvature and rigidity of ball packings. *Math. Res. Lett.*, 3(1):51–60, 1996.

[5] I. Izmestiev and J.-M. Schlenker. On the infinitesimal rigidity of polyhedra with vertices in convex position. arXiv:0711.1981v1, 2007.

[6] C. Lebrun. Einstein metrics and the Yamabe problem. In *Trends in mathematical physics (Knoxville, TN, 1998)*, volume 13 of *AMS/IP Stud. Adv. Math.*, pages 353–376. Amer. Math. Soc., Providence, RI, 1999.

Hyperbolization of ornaments

Jürgen Richter-Gebert, Martin von Gagern

1. What is hyperbolization?

While ornamental patterns based on the 17 Euclidean wallpaper groups are widely present in art and architecture, designs of similar ornaments based on hyperbolic symmetries are rare. The reason for this is twofold. First of all, the generation of hyperbolic ornamental patterns requires already a substantial knowledge or intuition in hyperbolic structures. Secondly, the technical process of rendering may be tedious (at least if performed by manual work) since it in principle requires the generation of infinitely many smaller and smaller objects.

We present a method that can be used to automatically transform an existing Euclidean ornamental pattern into a corresponding one with an underlying hyperbolic symmetry group. During this process we want to preserve as much as

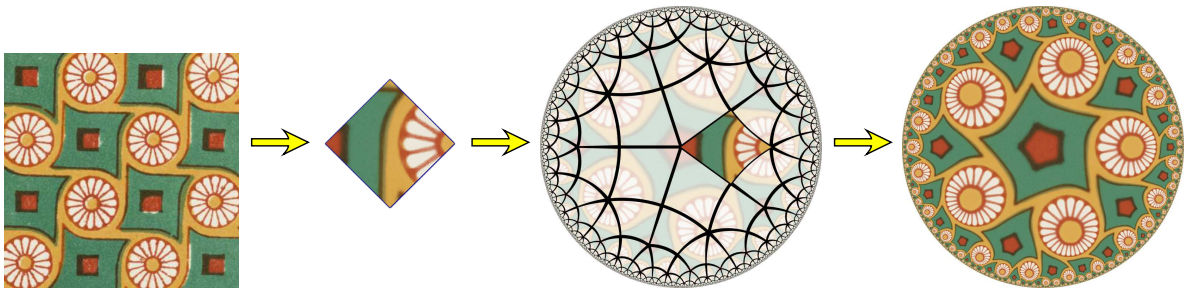

FIGURE 1. Transforming a scanned Euclidean input image to a hyperbolic ornament

possible from the original artistic input. Our process can be roughly divided into three steps:

Pattern recognition: Based on auto-correlation methods calculated via fast Fourier transformation we first analyze a Euclidean ornamental pattern. We extract its symmetry group and a fundamental region (see [1]).

Deformation: In a second step we deform the fundamental region such that we get a new region that could serve as fundamental region of a hyperbolic ornament. For this step we require only distortions of the pattern that are mathematically motivated, artistically reasonable and performable in reasonable time. We require the deformation to be a *conformal map*. This preserves the intersection angles of objects. Furthermore once the combinatorics is fixed a conformal map is uniquely determined. A detailed analysis is presented in [2].

Rendering: Finally, the deformed fundamental region is used to create the entire hyperbolic picture. To get a perfect rendering a *reverse pixel lookup* strategy is used that associates to every pixel of the final image a preimage in the central fundamental region (for details again see [2]).

2. HYPERBOLIZATION

We will exemplify the concept of hyperbolization in the relatively simple case of triangular reflection groups. Deformations of seven out of the 17 crystallographic groups can be reduced to this case (namely those with orbifold symbols 442, ∗442, 4∗2, 333, ∗333, 3∗3, 632, ∗632). The others groups have to be treated by slightly more advanced methods. Assume that we have an ornamental kaleidoscopic pattern based on a triangular reflection group for instance with corner angles $\frac{\pi}{2}$, $\frac{\pi}{4}$ and $\frac{\pi}{4}$. The fundamental region of this pattern is the triangle itself. The corner angles imply 2-fold, 4-fold and 4-fold rotational symmetry at the corners.

We want to conformally deform the triangle to a circular arc triangle (representing a hyperbolic triangle in the Poincaré disk model) such that the corner angles are other fractions of π (say $\frac{\pi}{2}$, $\frac{\pi}{4}$ and $\frac{\pi}{5}$). Riemann's mapping theorem guarantees that the map relating the two triangles is uniquely defined by conformality. In essence this map can be computed by a composition of Schwarz-Christoffel map (SCM) that maps the unit disk to the deformed triangle with an inverse SCM

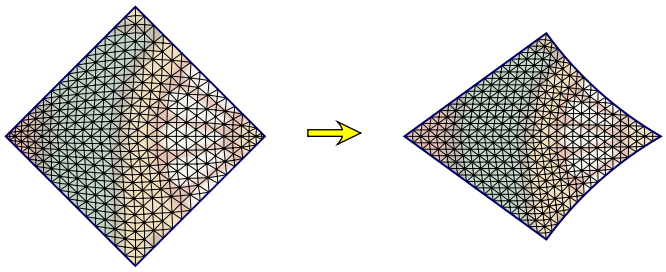

FIGURE 2. Deformation of a fundamental domain via discrete conformal maps

that maps the original triangle to the unit disk. This map can be extended to the Euclidean plane (punctured at the rotation centers) via the Schwarz reflection principle applied to the boundaries of the triangle.

3. Discrete conformal maps

Unfortunately, there is no known reasonably fast way to calculate the map described above. This is where Discrete Differential Geometry enters the stage. The concept of discrete conformal maps of a triangular mesh (as introduced by Bobenko, Pinkall, Schröder and Springborn [3]) is perfectly suited to calculate an approximation of the above map in reasonably short time using a variational principle. The method introduced there has several advantages that makes it perfectly suitable for applications in computer graphics. A discrete conformal map of a triangular mesh is defined by a collection of weights at the vertices. The edge lengths of the image mesh are related to the original mesh by scaling them according to the weights of the incident endpoints. Under successive refinement of the mesh this method approximates a smooth conformal map. The specification of target angle sums for the whole mesh allows an easy way to express the required changes to corner angles and flatness conditions elsewhere. A discrete conformal map can used as basis for a continuous interpolation of triangle interiors by assigning suitably chosen projective transformations to each of them. Here continuity is a consequence of the discrete conformality property. Figure 2 illustrates a discrete conformal map for a quadratic fundamental region from the Euclidean symmetry group 442 to the hyperbolic symmetry group 562. The Hyperbolic fundamental domain was approximated with a triangle mesh, which was then transformed to the corresponding Euclidean mesh.

4. The other groups

For the remaining (low symmetry) groups where all centers of rotation are at most two-fold, the symmetry type does not automatically fix the shape of the fundamental region. Thus also in the hyperbolization the exact shape of the deformed boundary is a priori unknown. As a consequence, the transformation has to start with an Euclidean mesh, and be performed in hyperbolic geometry to yield a conformally equivalent hyperbolic mesh. In general, straight boundary edges of

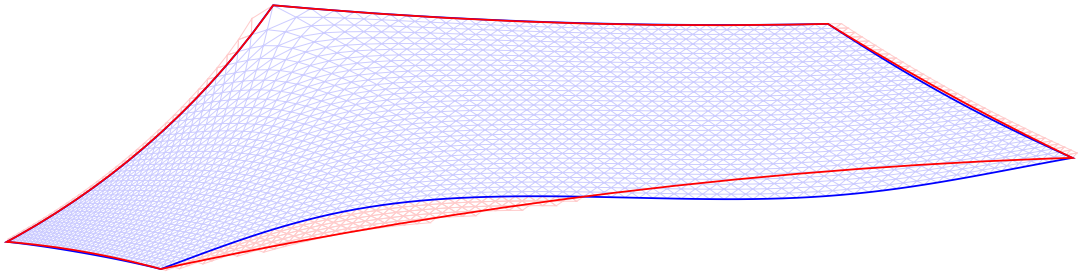

FIGURE 3. Straight edged hyperbolic fundamental region (red) and deformation of a straight edged Euclidean region (blue) for a low symmetry group

the Euclidean fundamental domain will *not* map to geodesics in the hyperbolic ornament. In this general case, any distinguished boundary curve will be straight in at most one world, as Figure 3 illustrates. This problem can be avoided by performing the deformation process directly on a triangle mesh of the orbifold, i.e., with corresponding edges identified, (see [2]). This approach avoids the problem of distinguished non-reflecting lines altogether.

REFERENCES

[1] M. VON GAGERN. *Computergestütztes Zeichnen in den Symmetriegruppen der euklidischen Ebene*. Diplomarbeit, TU München, 2007.

[2] J. RICHTER-GEBERT AND M. VON GAGERN. *Hyperbolization of Euclidean Ornaments*. SUBMITTED.

[3] B. SPRINGBORN, P. SCHRÖDER AND U. PINKALL. *Conformal equivalence of triangle meshes*. ACM SIGGRAPH, 2008.

Earthquakes on hyperbolic surfaces

JEAN-MARC SCHLENKER

(joint work with Francesco Bonsante and Kirill Krasnov)

Consider a closed surface S, of genus at least 2. A weighted multicurve on S is a disjoint union of simple closed curves $c_1, \dots, c_n$, each with a positive number w_i. Given a hyperbolic metric g on S, each c_i can be uniquely realized as a simple closed geodesic and those geodesics are disjoint. The fractional Dehn twist along a weighted multicurve is a surgery on hyperbolic metrics on S: one cuts (S, g) open along each of the c_i, rotates the right-hand side by w_i, and glues back (this does not depend on the orientation chosen for the c_i). This defines a map from the Teichmüller space $\mathcal{T}$ of S to itself.

Thurston showed that the space of weighted multicurves on S has a natural completion, the space $\mathcal{ML}$ of measured laminations on S. A geodesic measured lamination on (S, g) is a closed set which is a disjoint union of complete geodesics, endowed with a "transverse measure". Thurston also proved that map defined by

the notion of fractional Dehn twist extends continuously to the notion of earthquake on a measured lamination, therefore defining a map

$$E : \mathcal{ML} \times \mathcal{T} \to \mathcal{T} \ .$$

A neat property of this map is that it can be used to parameterize the Teichmüller space of S from a fixed point by the space of measured lamination, thanks to Thurston's Earthquake Theorem:

Theorem (Thurston)**.** *Let $g_0, g_1 \in \mathcal{T}$, there exists a unique $\lambda \in \mathcal{ML}$ such that $E(\lambda, g_0) = g_1$.*

A proof was given in [Ker83] and another one, based on anti-de Sitter geometry, in [Mes07].

A first extension concerns hyperbolic surfaces with conical singularities of angle less than π. For those surfaces the notion of measured lamination still makes perfect sense, and we proved with Francesco Bonsante [BS06] that given any two hyperbolic metrics with cone angles (with the same angles) there is a unique measured lamination λ such that the right earthquake on λ transforms one into the other.

A second extension, obtained with Francesco Bonsante and Kirill Krasnov [BKS06], applies to hyperbolic surfaces with geodesic boundary. Let $\mathcal{T}_{S,N}$ be the Teichmüller space of hyperbolic metrics with geodesic boundary on S with N disks removed (note that the length of the boundary components is not fixed). Let $\mathcal{ML}_{S,N}$ be the space of measured geodesic laminations on the interior of S for such a metric (that is, the weight of the lamination can accumulate close to the boundary). Then, given $g_0, g_1 \in \mathcal{T}_{S,N}$, there are exactly 2^N elements $\lambda \in \mathcal{ML}_{S,N}$ such that the right earthquake on λ sends g_0 to g_1.

The proof of both results uses the arguments of Mess' proof in [Mes07], but new twists are necessary. Instead of globally hyperbolic AdS manifolds as those considered in [Mes07], it is necessary to use corresponding manifolds with "particles" (cone singularities along time-like geodesics) for the statement on hyperbolic surfaces with cone singularities, and on multi-black holes (see e.g. [ÅBB$^+$98]) for the statement on surfaces with geodesic boundary. In both cases, it is necessary to understand the moduli spaces of the 3-dimensional metrics involved, as well as properties of their "convex cores".

References

[ÅBB$^+$98] Stefan Åminneborg, Ingemar Bengtsson, Dieter Brill, Sören Holst, and Peter Peldán. Black holes and wormholes in 2+1 dimensions. *Classical Quantum Gravity*, 15(3):627–644, 1998.

[BKS06] Francesco Bonsante, Kirill Krasnov, and Jean-Marc Schlenker. Multi black holes and earthquakes on Riemann surfaces with boundaries. arXiv:math/0610429 [math.GT], 2006.

[BS06] Francesco Bonsante and Jean-Marc Schlenker. AdS manifolds with particles and earthquakes on singular surfaces. *Geom. Funct. Anal.*, to appear. arXiv:math/0609116 [math.GT], 2006.

[Ker83] Steven P. Kerckhoff. The Nielsen realization problem. *Ann. of Math. (2)*, 117(2):235–265, 1983.

[Mes07] Geoffrey Mess. Lorentz spacetimes of constant curvature. *Geom. Dedicata*, 126:3–45, 2007.

Discrete square peg problem

Igor Pak

The *square peg problem* is beautiful and deceptively simple. It asks whether every Jordan curve $C \subset \mathbb{R}^2$ has four points which form a square. We call such squares *inscribed* into C.

The problem goes back to Toeplitz (1911), and over almost a century has been repeatedly rediscovered and investigated, but never completely resolved. By now it has been established for convex curves and curves with various regularity conditions, including the case of piecewise linear curves. While there are several simple and elegant proofs of the convex case, the piecewise linear case is usually obtained as a consequence of results proved by rather technical topological and analytic arguments. We present a simple proof in the piecewise linear case following Schnirelmann's ideas in [3]. Our proof follows [1, 2].

References

[1] I. Pak, *Lectures on Discrete and Polyhedral Geometry*, monograph to appear.

[2] I. Pak, Discrete Square Peg Problem, arXiv:0804.0657.

[3] L. G. Shnirelman, On certain geometrical properties of closed curves (in Russian), *Uspehi Matem. Nauk* **10** (1944), 34–44.

Volume and angle structures on 3-manifolds

Feng Luo

We propose an approach to find constant curvature metrics on triangulated closed 3-manifolds using a finite dimensional variational method whose energy function is the volume. The concept of an angle structure on a tetrahedron and on a triangulated closed 3-manifold is introduced. This follows the work of Casson, Murakami and Rivin who introduced the similar concept for ideal triangulations of compact 3-manifolds with torus boundary. It is proved by A. Kitaev and the author that any closed 3-manifold has a triangulation supporting an angle structure. The space of all angle structures on a triangulated 3-manifold is a bounded open convex polytope in a Euclidean space. The volume of an angle structure is defined by generalizing the Schläfli formula. Both the angle structure and the volume are natural generalizations of that of tetrahedra in the constant sectional curvature spaces and their volume. It is shown that the volume functional can be extended continuously to the compact closure of the moduli space, answering affirmatively a question of Milnor. In particular, the maximum point of the volume functional always exists in the compact closure of the space of angle structures. The main result shows that if the volume function on the space of angle structures has a local

maximum point, then either the manifold admits a constant curvature Riemannian metric or the triangulation supports a normal 2-sphere which intersects each edge in at most one point.

Extremal configurations of revolute-jointed robot arms

Ileana Streinu
(joint work with Ciprian S. Borcea)

A fundamental question in Robotics is the **Reach Problem**: *given a 3D revolute-jointed robot, compute the extremal values of the endpoint distance function and the corresponding extremal configurations.*

The most general type of revolute-jointed robot arms are the body-and-hinge chains: rigid bodies connected serially by hinges, as in Figure 1. Panel-and-hinge chains are a special case, with 2D panels instead of 3D bodies, i.e., consecutive hinges are coplanar. Polygonal chains with fixed edge lengths and fixed angles between consecutive edges can also be viewed as panel-and-hinge chains. A hinge is understood here as an entire line or turning axis, constraining the relative motion of two connected bodies to a rotation around their common hinge. We mark two points: the origin or start point s on the first body and the terminus t on the last body. We ask *what are the extremal values* of the distance function from s to t, as the chain takes all possible configurations (the boundaries of the bodies are immaterial and self-intersections are permitted). The problem was intensely studied in the 1980's, when a *necessary* condition for extremal configurations was recognized and proven in several papers [2, 3, 4, 6]: *the line joining the marked points must intersect all the hinges.* This incidence is understood projectively, that is, includes the possibility of parallelism, and the hinges are thought of as lines (not line segments).

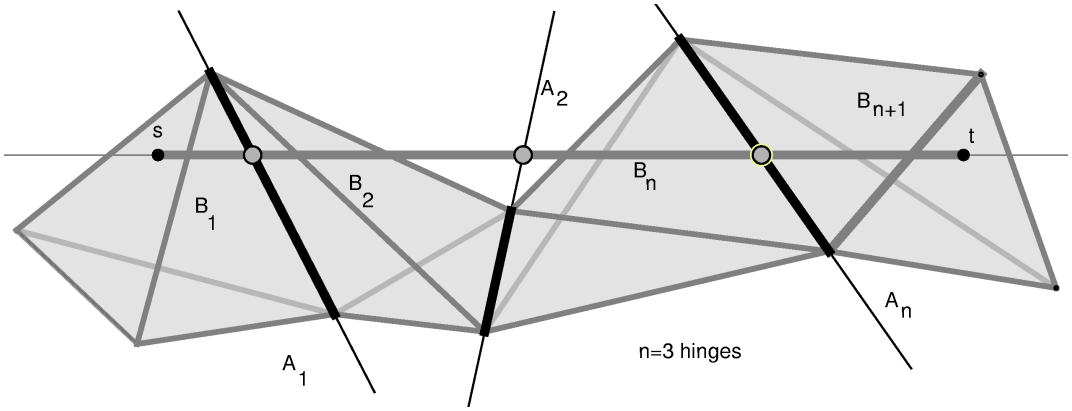

Figure 1. A body-and-hinge chain in R^3 with $n = 3$ hinges, four bodies (visualized as tetrahedra) and two marked points s and t on the end-bodies. In a maximum reach position, the axes meet the *oriented segment st* in the natural order.

This talk presented our recent results, giving an intrinsic, combinatorial characterization of the configurations attaining the global extremal values. The proofs work in arbitrary dimension d. The results are somewhat different for the global maximum and minimum, and for body-and-hinge as opposed to panel-and-hinge structures.

The *natural order* of the hinges is $1, 2, 3, \cdots$ as they appear on the chain. The *complement* of a line segment is with respect to the projective line containing the affine line segment, i.e., it goes through the point at infinity.

Theorem 1. ***(Global Maximum)*** *A body-and-hinge chain is in a global maximum configuration if and only if the segment from the origin s to the terminus t intersects all hinges* in their natural order. *Generically, the global maximum is attained in a unique configuration.*

Indeed, given a configuration satisfying this condition, we will mark in red the segment from s to t. In any other configuration of the chain, the red path appears as a polygonal chain in 3D, hence the endpoint distance will be shorter than in the straightened position. The necessity of the condition is obtained from a characterization of the global maximum as a global minimum of another function:

Theorem 2. ***(Global Maximum as a Global Minimum)*** *The global maximum of the endpoint distance function coincides with the length of the shortest path from s to t which meets all hinges in their natural order.*

The treatment of the minimum endpoint distance and minimal configurations is more specialized. When the endpoints can reach each other and the minimum distance is zero, an entire submanifold of critical values (rather than isolated points) occurs. Under suitable genericity assumptions, the endpoint squared distance function becomes a Morse-Bott function, leading to a formula for the Euler characteristic of the inverse kinematics solution space in terms of indices of critical configurations.

We derive an explicit formula for the Hessian, which is particularly useful for panel-and-hinge chains. In this case, we prove that local extrema are already global extrema, a fact which is not true for general body-and-hinge chains. Moreover:

Theorem 3. ***(Global Non-Zero Minimum)*** *A panel-and-hinge chain is in a global non-zero minimum configuration if and only if the complementary endpoint line segment oriented from the start point to the terminus meets the hinges in the natural order.*

Panel-and-hinge chains in critical configurations are subdivided into flat pieces connected at fold points: the endpoint axis cuts across the hinges in the flat regions, and goes through two consecutive hinges at fold points. When a panel-and-hinge chain is folded, the angles induced by the two incident hinges at a fold point and the constrained shortest path between the endpoints will satisfy a simple condition related to the triangle inequality on the sphere. At each fold point, the incident panels can be folded in two distinct ways. We obtain:

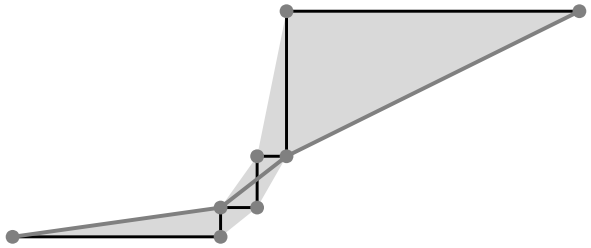

FIGURE 2. The shortest path between the chain endpoints gives the maximum reach value. The turning points of the path become the fold points in a 3D maximum configuration.

Theorem 4. ***(Number of Extremal Configurations)*** *Generically, the number of distinct extremal configurations is* 2^f*, where* f *is the number of fold points.*

These characterizations lead directly to elementary, surprisingly efficient algorithms for the four fundamental problems of robot arm reachability listed below, in the case of the class of panel-and-hinge satisfying the local criterion at the fold points. This class includes robot arms presented as polygonal chains with equal obtuse angles, including the orthogonal case. Until now, only numerical methods based on standard gradient descent methods were known.

(1) **Extremal distances:** compute the minimum and the maximum value of the endpoint distance function.
(2) **Extremal configurations:** compute one (or all) of the configurations that achieve the global minimum or maximum endpoint distance.
(3) **Motion Planning:** given an arbitrary configuration of the chain, reconfigure it to an extremal position: i.e., compute a trajectory in configuration space ending at an extremal configuration.
(4) **Optimized Motion Planning:** given a flat non-extremal configuration, reconfigure it in such a way that the distance function is monotone throughout the motion: decreases towards the minimum, or increases towards the maximum.

The first problem is solved using a shortest path calculation in an associated flat polygonal region, as in Figure 2. Fold angles are then computed and a maximum configuration is derived. To reconfigure from a flat position to a maximum configuration in a monotone fashion, we adapt Streinu's pseudo-triangulation algorithm [5] for the planar Carpenter's Rule Problem.

A more detailed theoretical development is presented in an arXiv preprint [1].

REFERENCES

[1] C. S. Borcea and I. Streinu. Extremal configurations of hinge structures. arXiv:0812.1375, Dec. 2008.
[2] S. Derby. The maximum reach of revolute jointed manipulators. *Mechanism and Machine Theory*, 16(3):255–261, 1981.
[3] A. Kumar and K. J. Waldron. The workspaces of a mechanical manipulator. *Journal of Mechanical Design*, 103(3):665–672, 1981.

[4] R. G. Selfridge. The reachable workarea of a manipulator. *Mechanism and Machine Theory*, 18(2):131–137, 1983.
[5] I. Streinu. Pseudo-triangulations, rigidity and motion planning. *Discrete and Computational Geometry*, 34(4):587–635, 2005.
[6] K. Sugimoto and J. Duffy. Determination of extreme distances of a robot hand - Part 1: A general theory. *Journal of Mechanical Design*, 103(3):631–636, 1981.

Discrete random interfaces

Richard Kenyon

We discussed a model of discrete two-dimensional interfaces in $\mathbb{R}^3$. These are piecewise-linear surfaces composed of translates of the faces of the unit cube, glued edge to edge, and with the property that the orthogonal projection to the plane $x+y+z=0$ is injective. These interfaces can be thought of as tilings of the plane with "lozenges", that is, with 60° rhombi. Given a closed curve in $\mathbb{Z}^3$ which can be spanned by such an interface, consider the uniform probability measure on the set of all such spanning interfaces. There is a law of large numbers, proved by Cohn, myself and Propp [1], which says that for a fixed "wire frame" boundary curve γ, in the limit that the lattice spacing tends to zero the uniform random interface will concentrate on a nonrandom limit shape, which is a continuous surface spanning γ. The limiting surface can be obtained through a variational principle, essentially maximizing a local entropy functional. Here the local entropy is a function only of the slope of the interface, and is just the exponential growth rate of interfaces having average slope in that direction.

Techniques of Kasteleyn show how to compute explicitly the entropy function as a function of slope, and the resulting formula is very simple: when the normal to the interface has (positive) coordinates (p_x, p_y, p_z), the growth rate is proportional to the volume of the idea hyperbolic 3-simplex with dihedral angles proportional to (p_x, p_y, p_z).

In work with Okounkov [2] we were able to solve explicitly the corresponding PDE for the limit interface, reducing it to the complex Burgers' equation. This permits parameterization of solutions with analytic functions.

Many related interface models, associated with underlying dimer models, have very similar solutions [3, 2].

References

[1] H. Cohn, R. Kenyon, J. Propp, A variational principle for domino tilings, *J. Amer. Math. Soc.*, **14** (2001), no. 2, 297–346.
[2] R. Kenyon, A. Okounkov, Limit shapes and the complex Burgers equation, *Acta Math.* **199** (2007), 263–302.
[3] R. Kenyon, A. Okounkov, S. Sheffield, Dimers and amoebae. *Ann. of Math.* (2) **163** (2006), no. 3, 1019–1056.

The Pentagram map: a discrete integrable system

Serge Tabachnikov
(joint work with Valentin Ovsienko, Richard Schwartz [2, 3])

Given a convex n-gon P in the projective plane, let $T(P)$ be the convex hull of the intersection points of consecutive shortest diagonals of P. The map T is the pentagram map. The pentagram map commutes with projective transformations. Let C_n be the space of convex n-gons modulo projective transformations. Then the pentagram map induces a self-diffeomorphism $T : C_n \to C_n$.

T is the identity map on C_5 and an involution on C_6, see [5]. Experimentally, for $n \geq 7$, the orbits of T on C_n exhibit the kind of quasi-periodic motion associated to a completely integrable system: T preserves a certain foliation of C_n by roughly half-dimensional tori, and the action of T on each torus is conjugate to a rotation. A conjecture in [6] that T is completely integrable on C_n is still open, but we are very close to proving it.

A *twisted n-gon* is a map $\phi : \mathbb{Z} \to \mathbb{RP}^2$ such that $\phi(n+k) = M \circ \phi(k)$ for all $k \in \mathbb{Z}$ and some fixed element $M \in PGL(3, \mathbb{R})$ called the *monodromy*. Set $v_i = \phi(i)$ and assume that v_{i-1}, v_i, v_{i+1} are in general position for all i. Let P_n be the space of twisted n-gons modulo projective equivalence. We show that the pentagram map $T : P_n \to P_n$ is completely integrable in the classical sense of Arnold–Liouville. We give an explicit construction of a T-invariant Poisson structure and complete list of Poisson-commuting integrals for the map.

We apply this result to *universally convex* twisted n-polygons. These are polygons for which the map ϕ is such that $\phi(\mathbb{Z}) \subset \mathbb{R}^2 \subset \mathbb{RP}^2$ is convex and contained in the positive quadrant, and the monodromy $M : \mathbb{R}^2 \to \mathbb{R}^2$ is a diagonal linear transformation with eigenvalues $0 < a < 1 < b$. The image of ϕ looks somewhat like a "polygonal hyperbola". Denote by U_n the space of universally convex twisted n-gons modulo projective equivalence.

Theorem. *Almost every point of U_n lies on a smooth torus that has a T-invariant affine structure. The orbit of almost every universally convex n-gon undergoes quasi-periodic motion under the pentagram map.*

We associate to every vertex v_i two numbers:

$$x_i = [v_{i-2},\, v_{i-1},\, ((v_{i-2}, v_{i-1}) \cap (v_i, v_{i+1}))\,,\, ((v_{i-2}, v_{i-1}) \cap (v_{i+1}, v_{i+2}))]$$
$$y_i = [((v_{i-2}, v_{i-1}) \cap (v_{i+1}, v_{i+2}))\,,\, ((v_{i-1}, v_i) \cap (v_{i+1}, v_{i+2}))\,,\, v_{i+1},\, v_{i+2}],$$

see Figure 1, where the bracket is the cross ratio of 4 points in $\mathbb{RP}^1$ given by

$$[t_1, t_2, t_3, t_4] = \frac{(t_1 - t_2)\,(t_3 - t_4)}{(t_1 - t_3)\,(t_2 - t_4)}$$

in an affine parameter t. We call these coordinates the *corner invariants*.

The pentagram map is described in these coordinates as follows:

$$T^* x_i = x_i \,\frac{1 - x_{i-1}\, y_{i-1}}{1 - x_{i+1}\, y_{i+1}}, \qquad T^* y_i = y_{i+1}\,\frac{1 - x_{i+2}\, y_{i+2}}{1 - x_i\, y_i}.$$

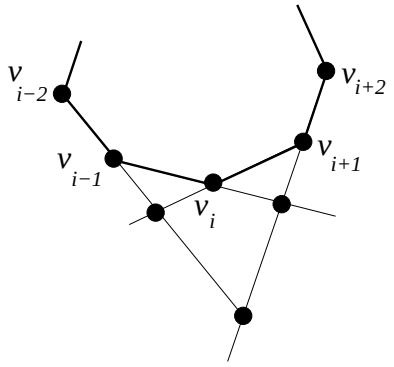

FIGURE 1. Points involved in the definition of the corner invariants.

Consider the *rescaling operation* given by

$$R_t : \quad (x_1, y_1, ..., x_n, y_n) \to (tx_1, t^{-1}y_1, ..., tx_n, t^{-1}y_n).$$

It follows that the pentagram map commutes with the rescaling operation. Let

$$O_n = \prod_{i=1}^{n} x_i\,, \quad E_n = \prod_{i=1}^{n} y_i\,, \quad O_{n/2} = \prod_{i \text{ even}} x_i + \prod_{i \text{ odd}} x_i\,, \quad E_{n/2} = \prod_{i \text{ even}} y_i + \prod_{i \text{ odd}} y_i,$$

the latter two when n is even. These functions are invariant under the pentagram map. Let ϕ be a twisted n-gon with invariants $x_1, y_1, ...$, and let M be the monodromy. Lift M to an element of $GL_3(\mathbb{R})$. Then

$$\Omega_1 = \frac{\text{trace}^3(M)}{\det(M)}; \qquad \Omega_2 = \frac{\text{trace}^3(M^{-1})}{\det(M^{-1})};$$

depend only on the conjugacy class of M. Set: $\widetilde{\Omega}_1 = O_n^2 E_n \Omega_1, \widetilde{\Omega}_2 = O_n E_n^2 \Omega_2$. In [6] it is shown that $\widetilde{\Omega}_1$ and $\widetilde{\Omega}_2$ are polynomials in the corner invariants. Since the pentagram map preserves the monodromy, and O_n and E_n are invariants, the two functions $\widetilde{\Omega}_1$ and $\widetilde{\Omega}_2$ are also invariants. Consider the decomposition into homogeneous components with respect to the scaling:

$$\widetilde{\Omega}_1 = \sum_{k=1}^{[n/2]} O_k; \qquad \widetilde{\Omega}_2 = \sum_{k=1}^{[n/2]} E_k$$

where O_k has weight k and E_k has weight $-k$. It follows that the functions $O_1, E_1, O_2, E_2, ...$ are integrals of the pentagram map. These are the *monodromy invariants*. In [6] it is shown that the monodromy invariants are algebraically independent.

The Poisson bracket on P_n is as follows:

$$\{x_i, x_{i\pm1}\} = \mp x_i\, x_{i+1}, \qquad \{y_i, y_{i\pm1}\} = \pm y_i\, y_{i+1},$$

and all other brackets of coordinates functions vanish. The main lemmas concerning the Poisson bracket are:

(1) The Poisson bracket is invariant with respect to the Pentagram map.
(2) The monodromy invariants Poisson commute.

(3) The invariants O_n, E_n and, in the even case, $O_{n/2}, E_{n/2}$, are Casimir functions.
(4) The Poisson bracket has corank 2 if n if odd and corank 4 if n is even.

These results imply that P_n is foliated by symplectic leaves which carry a leafwise T-invariant Lagrangian foliation. The leaves of a Lagrangian foliation carry a canonical affine structure, in which T is a parallel translation, cf. [1]. For universally convex twisted n-gons, the leaves are compact, and hence tori. This implies the theorem.

We also consider the continuous limit $n \to \infty$ of a twisted n-gon as a smooth twisted non-degenerate parametrized curve $\gamma : \mathbb{R} \to \mathbb{R}\mathrm{P}^2$ such that $\gamma(x+1) = M(\gamma(x))$, for all $x \in \mathbb{R}$ and a fixed $M \in PGL(3, \mathbb{R})$. As in the discrete case, we consider classes of projectively equivalent curves.

It is well known that the space of non-degenerate twisted curves is in one-to-one correspondence with the space of linear differential operators

$$A = \left(\frac{d}{dx}\right)^3 + u(x)\,\frac{d}{dx} + v(x),$$

where u and v are smooth periodic functions, see [4].

The construction of a continuous analog of the map T is as follows. Given a non-degenerate curve $\gamma(x)$, at each point x draw the chord $(\gamma(x-\varepsilon), \gamma(x+\varepsilon))$ and obtain a new curve, $\gamma_\varepsilon(x)$, as the envelop of these chords. Let u_ε and v_ε be the respective periodic functions. It turns out that

$$u_\varepsilon = u + \varepsilon^2 \widetilde{u} + (\varepsilon^3), \quad v_\varepsilon = v + \varepsilon^2 \widetilde{v} + (\varepsilon^3),$$

giving the curve flow: $\dot{u} = \widetilde{u},\ \dot{v} = \widetilde{v}$. Excluding v yields

$$\ddot{u} + \frac{\left(u^2\right)''}{6} + \frac{u^{(IV)}}{12} = 0,$$

which is the classical Boussinesq equation. Thus the pentagram map is a discretization of the Boussinesq equation.

References

[1] V. Arnold. Mathematical Methods of Classical Mechanics, Springer-Verlag, New York, 1989.
[2] V. Ovsienko, R. Schwartz, S. Tabachnikov. *The Pentagram Map: a discrete integrable system*, preprint 2008.
[3] V. Ovsienko, R. Schwartz, S. Tabachnikov. *Quasiperiodic Motion for the Pentagram Map*, preprint 2009.
[4] V. Ovsienko, S. Tabachnikov, Projective differential geometry old and new, from Schwarzian derivative to the cohomology of diffeomorphism groups, Cambridge University Press, Cambridge, 2005.
[5] R. Schwartz, *The Pentagram Map*, Experimental Math. **1** (1992), 71–81.
[6] R. Schwartz, *Discrete Monodromy, Pentagrams, and the Method of Condensation* J. Fixed Point Theory Appl. **3** (2008), 379–409.

Piecewise linear saddle spheres on $\mathbb{S}^3$

Gaiane Panina

By $S^3 \subset \mathbb{R}^4$ we denote the unit sphere centered at the origin O. A *plane on the sphere* S^3 is a plane in the sense of spherical geometry. A closed surface Γ immersed in S^3 is called *saddle* if no plane intersects Γ locally at just one point.

Definition. A *piecewise linear saddle sphere* (a *PLS-sphere*, for short) on S^3 is an immersed piecewise linear surface which is homeomorphic to S^2. We assume in addition that a PLS-sphere does not coincide with a plane, that all its edges are shorter than π, and that its vertex-edge graph is 3-connected.

A PLS-sphere is called *elementary Barner* if there is a point $p \in S^3$ such that each great semicircle with endpoints p and $-p$ hits the surface exactly once.

The interplay between PLS-spheres and smooth saddle spheres is not well understood. On the one hand, it seems plausible that a piecewise linear saddle sphere can be approximated by a smooth saddle sphere and vice versa. On the other hand, there is just one proven result (see [7]). It asserts that an elementary Barner PLS-sphere with a trivalent vertex-edge graph has a C^∞-smooth saddle approximation.

Definition. A face f of a PLS-sphere Γ is called *an inflexion face* if
(1) f is bounded by two convex broken lines (say, by L_1 and L_2) such that the convexity directions look like in Figure 1,
(2) all the edges of L_1 are convex, whereas all the edges of L_2 are concave.

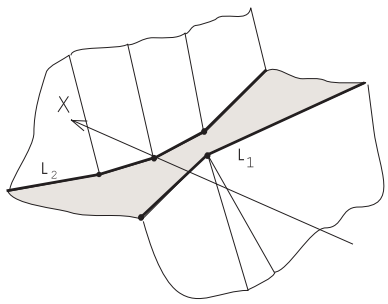

Figure 1. An inflexion face.

Definition. A face f of a PLS-sphere Γ is called *a reflex face* if its supplement fits an open hemisphere.

We announce here the following result:

Theorem.
(1) Each immersed saddle sphere $\Gamma \subset S^3$ belongs to one of the following disjoint classes:
(a) Γ has at least two reflex faces.
(b) Γ has exactly one reflex face and at least two inflexion faces.

(c) Γ has no reflex faces and at least 4 inflexion faces.

(2) There are no embedded PLS-spheres on S^3 of type (a).

(3) There are no embedded PLS-spheres on $\mathbb{R}P^3$.

(4) There exist immersed PLS-spheres on $\mathbb{R}P^3$.

(5) There exist elementary Barner PLS-spheres of type (c). Moreover, the set of elementary Barner PLS-spheres with any fixed number of inflexion faces (greater than 3) is non-empty and disconnected.

Sketch of the proof. Given an oriented PLS-sphere, we can speak of its *convex and concave* edges. We paint all the convex (respectively, concave) edges red (respectively, blue).

Combinatorially, a PLS-sphere is a planar graph with additional equipment: its edges are colored and some of the angles (the reflex ones) are marked. (Some similar phenomena are studied in [3] and [4].)

Definition. For a face f of a PLS-sphere, we algorithmically define its *index* $i(f)$:

(1) At the beginning, put $i(f) := 0$. Start going along the boundary of the face f.

(2) Once we pass by a vertex at which the color changes, put $i(f) := i(f) + 1$.

(3) Once we pass by a vertex, if the color does not change and the angle we are passing by is not reflex, put $i(f) := i(f) + 2$. (If the color does not change and the angle is reflex, we keep $i(f)$ unchanged.)

Some counts based on a discrete version of Segre's Theorem yield that one of the following cases holds:

(1) Γ has at least two faces with $i(f) = 0$.

(2) Γ has one face with $i(f) = 0$ and at least two faces with $(f) = 2$

(3) Γ has no faces with $i(f) = 0$ and at least 4 faces with $i(f) = 2$.

This yields statement (1) of the Theorem. The statements (2–4) follow from (1), whereas (5) is proven in [5, 7]. □

Motivations.

- The proof of the Theorem is based on and generalizes the Segre's Theorem: *Let a closed smooth simple curve $c \subset S^2$ have a non-empty intersection with any great semicircle. Then c has at least 4 inflexion points.*
- There exist embedded saddle tori on $\mathbb{R}P^3$. V. I. Arnold [2] formulated some conjectures about them (and about their higher dimensional versions). Some of the conjectures proved to be wrong [6], but two of them still stand open for $\mathbb{R}P^3$. In particular, he conjectured that the set of all smooth embedded saddle tori on $\mathbb{R}P^3$ is connected (compare with Theorem, (5)).
- Smooth elementary Barner saddle spheres arose originally in a relationship (see [5, 7]) to the following uniqueness conjecture proven for analytic surfaces by A. D. Alexandrov in [1]:

  Let $K \subset \mathbb{R}^3$ be a smooth convex body. If for a constant C, at every point of ∂K, we have $R_1 \le C \le R_2$, then K is a ball. (R_1 and R_2 stand for the principal curvature radii of ∂K).

Here is the link: Let K be a counterexample to the conjecture. Denote by h_K its support function and denote by h_C the support function of the ball of radius C. The graph γ of the difference $h_K - h_C$ is a conical surface in $\mathbb{R}^4$ with the apex at the origin O. Its intersection with S^3 is an elementary Barner saddle sphere.

Vice versa, a smooth elementary Barner saddle sphere spans a cone in $\mathbb{R}^4$ which can be interpreted as the graph of some positively homogeneous function h. For a sufficiently large C, the sum $h + h_C$ is a convex function. Then it is a support function of some convex body K which is a counterexample to the conjecture.

References

[1] A. D. Alexandrov, *On uniqueness theorems for closed surfaces.* (Russian) Doklady Akad. Nauk SSSR 22 (1939) no. 3, 99–102.

[2] V. Arnold, *Ramified covering $CP^2 \to S^4$, hyperbolicity, and projective topology*, Siberian Math. J. 29 (1988) no. 5, 36–47.

[3] S. Gortler, C. Gotsman, D. Thurston, *Discrete one-forms on meshes and applications to 3D mesh parameterization*, Comput. Aided Geom. Design 23 (2006) no. 2, 83–112.

[4] R. Haas, D. Orden, G. Rote, F. Santos, B. Servatius, H. Servatius, D. Souvaine, I. Streinu, and W. Whiteley, *Planar minimally rigid graphs and pseudotriangulations*, J. Comput. Geom. 31 (2005) no. 1–2, 31–61.

[5] Y. Martinez-Maure, *Contre-exemple à une caractérisation conjecturée de la sphère*, C. R. Acad. Sci. Paris Sér. I Math. 332 (2001) no. 1, 41–44.

[6] S. Orevkov, *A la recherche de la topologie projective. Du cote de chez Arnold.* Talk on the International Conference "Arnold-70", Moscow, August 20–25, 2007.

[7] G. Panina, *New counterexamples to A. D. Alexandrov's uniqueness hypothesis*, Advances in Geometry 5 (2005) no. 2, 301–317.

Discrete conformal equivalence for triangle meshes

Boris Springborn

(joint work with A. I. Bobenko, U. Pinkall, P. Schröder)

Two Riemannian metrics g and $\tilde{g}$ on a smooth 2-manifold M (possibly with boundary) are conformally equivalent if $\tilde{g} = e^{2u} g$ for some $u : M \to \mathbb{R}$. This means that infinitesimal lengths are scaled by a conformal factor e^u which does not depend on direction but only on position. In this talk, we explore a straightforward discretization of this concept of conformal equivalence [1]. Instead of smooth surfaces we consider surface triangulations, and instead of Riemannian metrics g we consider functions ℓ on the set of edges which assign to each edge ij a length ℓ_{ij} in such a way that the triangle inequalities are satisfied for all triangles of the triangulation. We consider two such discrete metrics ℓ and $\tilde{\ell}$ as *discretely conformally equivalent* if a conformal factor e^{u_i} can be associated to each vertex i such that for all edges ij

$$\tilde{\ell}_{ij} = e^{(u_i+u_j)/2} \ell_{ij}.$$

In terms of the logarithmic edge lengths $\lambda = 2\log\ell$, this relation is linear:

$$\tilde{\lambda}_{ij} := \lambda_{ij} + u_i + u_j. \tag{1}$$

Edge lengths $\tilde{\ell}_{ij}$ determine triangle angles. Let $\tilde{\alpha}^k_{ij}$ be the angle at vertex k in triangle ijk with edge lengths $\tilde{\ell}_{ij}$, $\tilde{\ell}_{jk}$, $\tilde{\ell}_{ki}$, and let $\widetilde{\Theta}_k = \sum_{ijk\ni k} \tilde{\alpha}^k_{ij}$ be the sum of angles around vertex k. We consider the following problem:

Given (i) a triangulation with a discrete metric ℓ, and *(ii)* a desired angle sum $\widehat{\Theta}_k$ for each vertex k, *find* a discretely conformally equivalent metric $\tilde{\ell}$ that has at each vertex the desired angle sum, that is, $\widetilde{\Theta}_k = \widehat{\Theta}_k$ for each vertex k. In particular, we are interested in the case where the desired angle sum $\widehat{\Theta}_k$ equals 2π for all interior vertices k. In this case, the problem asks for a discretely conformally equivalent flat metric with prescribed total angles at the boundary vertices (discrete conformal flatterning problem).

Analytically, the above problem amounts to one non-linear equation per vertex in the variables u_i, which are also associated to the vertices. It turns out that these equations are variational: The discrete metric $\tilde{\ell}$ solves the problem if and only if u is a critical point of the function

$$S(u) = \sum_{ijk} \left(2f\left(\tfrac{1}{2}\tilde{\lambda}_{ij}, \tfrac{1}{2}\tilde{\lambda}_{jk}, \tfrac{1}{2}\tilde{\lambda}_{ki}\right) - \pi(u_i + u_j + u_k)\right) + \sum_i \widehat{\Theta}_i u_i,$$

where the first sum is taken over all triangles ijk of the triangulation, the second sum is taken over all vertices i, the $\tilde{\lambda}_{ij}$ are defined by equation (1) as functions of u, and the function $f(x_1, x_2, x_3)$ is defined as follows: If x_1, x_2, x_3 are real numbers such that there exists a Euclidean triangle with sides e^{x_1}, e^{x_2}, e^{x_3}, then let α_1, α_2, α_3 be the opposite angles, and define

$$f(x_1, x_2, x_3) = \alpha_1 x_1 + \alpha_2 x_2 + \alpha_3 x_3 + \text{Л}(\alpha_1) + \text{Л}(\alpha_2) + \text{Л}(\alpha_3),$$

where $\text{Л}(\alpha) = -\int_0^\alpha \log|2\sin t|\, dt$ is Milnor's Lobachevsky function [2]. It turns out that $\frac{\partial f}{\partial x_i} = \alpha_i$, and therefore $\frac{\partial S}{\partial u_i} = \widehat{\Theta}_i - \widetilde{\Theta}_i$, which proves the claim about the critical points of $S(u)$.

The above definition of $f(x_1, x_2, x_3)$ assumes that e^{x_1}, e^{x_2}, e^{x_3} satisfy the triangle inequalities. Otherwise, a triangle with these sides does not exist and the angles α_1, α_2, α_3 are not defined. However, the definition of f can be extended to all of $\mathbb{R}^3$ by setting the angles to 0, 0, π whenever a triangle inequality is violated, where the value π is assigned to the angle opposite the side that is too long. If f is extended in this way, it is still continuously differentiable and convex. (It is strictly convex in the original domain and linear outside.) In fact, the extended function f is (up to a factor of π) the Ronkin function of the polynomial $z_1 + z_2 + z_3$:

$$\tfrac{1}{\pi} f(x_1, x_2, x_3) = (\tfrac{1}{2\pi i})^3 \iiint_{S^1(e^{x_1})\times S^1(e^{x_2})\times S^1(e^{x_3})} \log\left|z_1 + z_2 + z_3\right| \tfrac{dz_1}{z_1} \wedge \tfrac{dz_2}{z_2} \wedge \tfrac{dz_3}{z_3}.$$

(This Ronkin function also played an important role in Rick Kenyon's talk.)

With f extended in this way, the function $S(u)$ is convex and defined on $\mathbb{R}^{(\#\text{vertices})}$. This reduces the discrete conformal flattening problem to an unconstrained convex optimization problem which is easy enough to solve numerically to render this approach useful for practical applications [3].

The fact that Milnor's Lobachevsky function appears in the variational principle indicates that there should be some connection with hyperbolic geometry. Indeed, the discrete conformal flattening problem is equivalent with the following one [4]: *Given* a surface with complete hyperbolic metric with cusps, *find* a hyperbolic polyhedron with vertices at infinity whose boundary is isometric to the given surface. The same variational principle can also be used to solve this problem.

References

[1] Feng Luo. Combinatorial Yamabe flow on surfaces. *Commun. Contemp. Math.* 6:5 (2004), 765–780.

[2] John Milnor. Hyperbolic geometry: the first 150 years. *Bull. Amer. Math. Soc. (NS)* 6:1 (1982), 9–24.

[3] Boris Springborn, Peter Schröder, and Ulrich Pinkall. Conformal equivalence of triangle meshes. *ACM Transactions on Graphics* 27:3. [Proceedings of ACM SIGGRAPH '08]

[4] Alexander I. Bobenko, Ulrich Pinkall, and Boris Springborn. Discrete conformal equivalence and ideal hyperbolic polyhedra. In preparation.

Open problems in Discrete Differential Geometry

Collected by Günter Rote

Problem 1 (Günter M. Ziegler)**.** What is the smallest possible maximum vertex degree $f(d)$ for a centrally symmetric triangulation of the d-sphere? (Or a simplicial $(d+1)$-polytope.) The known bounds are $f(1) = 2$, $f(2) = 4$, and $d+1 < f(d) \leq 2d$. The upper bound comes from the cross-polytope. If one could show $f(d) < 3d/2$ for some large d that would have interesting consequences.

Problem 2 (Richard Kenyon)**.** Let M be a closed polyhedral surface homeomorphic to S^2 which is entirely composed of equal regular pentagons. If M is immersed in 3-space, is it necessarily the boundary of a union of solid dodecahedra that are glued together at common facets? The pentagonal faces may intersect each other (and the "union of solid dodecahedra" must be defined appropriately) but two different faces are not allowed to coincide. (The corresponding question for equal *squares* has an affirmative answer.)

Note (Ulrich Brehm): The great dodecahedron (Kepler-Poinsot polyhedron) is an interesting example, but it has genus 4. Moreover, the vertex-figures are self-crossing pentagrams, and therefore the surface is not immersed. The question would be interesting even for immersions of arbitrary closed surfaces, and for orientable closed surfaces of genus smaller than four where arbitrary selfintersecctions are allowed.

Problem 3 (Wolfgang Kühnel)**.** Let M^d be a triangulated d-manifold (simply connected, closed) with a discrete metric such that the discrete curvature (angle defect) along any $(d-2)$-simplex is positive. Give a *discrete* proof that M^d is homeomorphic to S^d. (Or give a counterexample.)

For $d = 3$, recent unpublished work of Matveev/Shevshichin verifies this by explicitly smoothing the metric; presumably the smoothing could also be done using Ricci flow. See also earlier work of Cheeger for general dimensions.

Note: Nonnegative curvature is not sufficient, as demonstrated by a flat torus. $\mathbb{C}P^2$ has a metric of positive sectional curvature, but the polyhedral condition should correspond to the stronger condition of positive curvature operator.

Problem 4 (Joseph O'Rourke)**.** Can a finite number of disjoint (closed) line segments in the plane, acting as 2-sided mirrors, and a point light source be arranged so that no light ray escapes to infinity? It seems most natural to treat the mirrors as open segments, but they should be disjoint when closed. The conjecture is that this is impossible.

Problem 5 (Günter Rote)**.** Take the complete graph K_4 embedded in the plane in general position, with vertices p_1, p_2, p_3, p_4. Pick two arbitrary points a and b and define two functions ω_{ij} and f_{ij} on the six edges of this graph:

$$\omega_{ij} := \frac{1}{[p_i p_j p_k][p_i p_j p_l]}, \qquad f_{ij} := [a p_i p_j][b p_j p_j], \tag{1}$$

where k and l are the two vertices different from i and j, and $[q_1 q_2 \dots q_n]$ denotes signed area of the polygon $q_1 q_2 \dots q_n$. (The function ω_{ij} is a *self-stress*: the equilibrium condition $\sum_j \omega_{ij}(p_j - p_i) = 0$ holds for every vertex i, where the summation is over all edges ij incident to i.) Then we have the following identity:

$$\sum_{1 \le i < j \le 4} \omega_{ij} f_{ij} = 1 \tag{2}$$

This generalizes to any wheel (graph of a pyramid) with a vertex p_0 that is connected to vertices $p_1, \dots, p_n$ forming a cycle, with the self-stress

$$\omega_{i,i+1} := \frac{1}{[p_i p_{i+1} p_0][p_1 p_2 \dots p_n]}, \qquad \omega_{0,i} := \frac{[p_{i-1} p_i p_{i+1}]}{[p_{i-1} p_i p_0][p_i p_{i+1} p_0][p_1 p_2 \dots p_n]}.$$

(The summation in (2) extends over all edges of the graph.) A different formula for f_{ij} that fulfills (2) is given by a line integral over the segment $p_i p_j$:

$$f'_{ij} := \tfrac{3}{2} \cdot \|p_i - p_j\| \cdot \int_{x \in p_i p_j} \|x\|^2 \, ds = \tfrac{1}{2} \cdot \|p_i - p_j\|^2 \cdot \left(\|p_i\|^2 + \|p_j\|^2 + \langle p_i, p_j \rangle \right)$$

Question 1: Are there other graphs with n vertices and $2n-2$ edges, for which a self-stress ω satisfying (2) can be defined? The next candidates with 6 vertices are the graph of a triangular prism with an additional edge, and the complete bipartite graph $K_{3,3}$ with an additional edge.

Question 2: Are these formulas an instance of a more general phenomenon? What are the connections to homology and cohomology?

Question 3: By positive scaling of the function f given by (1) or by adding a function that is orthogonal to the space of self-stresses (i. e., it lies in the range of the rigidity map), one obtains different functions f for which the expression in (2) is positive, see [1, Lemma 3.10]. Are all functions f that assign a number to each segment in the plane and that make (2) positive for all embeddings of K_4 obtained in this way?

[1] Günter Rote, Francisco Santos, and Ileana Streinu, *Expansive motions and the polytope of pointed pseudo-triangulations*, in: Discrete and Computational Geometry—The Goodman-Pollack Festschrift, Springer, 2003, pp. 699–736, arXiv:math/0206027 [math.CO].

Problem 6 (Jürgen Richter-Gebert)**.** Take $2 \cdot 5 = 10$ vectors A, B, C, D, E and A', B', C', D', E' in $\mathbb{C}^2$. Consider 2×2 determinants $[AB]$ etc. Take the quotient

$$\alpha(A, B, C, D, E|A', B', C', D', E') := \frac{[AB][BC][CD][DE][EA]}{[A'B'][B'C'][C'D'][D'E'][E'A']}$$

The alternating sum of α over all 4! simultaneous permutations of $A \dots E$ and $A' \dots E'$ that start with A/A' is 0. This should also be true for a general number of $2n$ points. Thus we conjecture in [1]:

Let $A_1, \dots, A_n, A'_1, \dots, A'_n \in \mathbb{K}^2$ be $2n$ points in a 2-dimensional vector space over a commutative field $\mathbb{K}$. Then the following formula holds

$$\sum_{\pi=(1,\pi_2,\dots,\pi_n)\in S_n} \sigma(\pi)\alpha(\pi(A_1, \dots, A_n)|\pi(A'_1, \dots, A'_n)) = 0.$$

where $\alpha(A_1, , \dots, A_n|A'_1, , \dots, A'_n)$ is a cyclic quotient analogous to the above one.

(This follows trivially from symmetry arguments for $n = 3, 4, 7, 8, 11, 12, \dots$, has been proved for 5 and 6, and seems true for 9 and 10.)

[1] Alexander Below, Jürgen Richter-Gebert, Vanessa Krummeck, *Complex matroids, phirotopes and their realizations in rank 2*, in: Discrete and Computational Geometry—The Goodman-Pollack Festschrift, Springer, 2003, pp. 203–233.

Problem 7 (Ivan Izmestiev)**.** An embedded graph in S^3 is called *linked* if it contains two disjoint linked cycles. Is there a convex 4-polytope P such that its 1-skeleton $P^{(1)}$ is linked as a graph in $\partial P \approx S^3$, but has a different embedding that is not linked?

Background: Let G be a graph with Colin de Verdière invariant $\mu(G) = 4$, and let M be a Colin de Verdière matrix for G. According to a conjecture of [1] and [2], the null-space of M yields then a non-linked embedding of G.

The positive solution of the problem would disprove this conjecture: Since $G = P^{(1)}$ has a non-linked embedding, $\mu(G) = 4$. By [3], there is a Colin de Verdière matrix M whose null-space represents G as the skeleton of P, and thus in a linked way.

[1] László Lovász, Alexander Schrijver, *On the null space of a Colin de Verdière matrix*, Symposium à la Mémoire de François Jaeger (Grenoble, 1998). Ann. Inst. Fourier (Grenoble) **49** (1999), no. 3, 1017–1026.

[2] László Lovász, *Steinitz representations of polyhedra and the Colin de Verdière number*, J. Combin. Theory Ser. B **82** (2001), no. 2, 223–236.

[3] Ivan Izmestiev, *Colin de Verdière number and graphs of polytopes*, to appear in Israel J. Math., arXiv:0704.0349 [math.CO].

Problem 8 (Serge Tabachnikov)**.** The standard origami model of a hyperbolic paraboloid is made from a square paper, folded zig-zag along many concentric squares and along the two diagonals. What is really going on in this model? Can it be realized with straight creases and with (developable) faces that are isometric to plane faces, or does it necessarily involve some stretching of the paper?

Problem 9 (Serge Tabachnikov)**.** We are given a partition of the unit square into T triangles (not necessarily a triangulation). A vertex that lies on an edge of some triangle or of the bounding square has 1 degree of freedom, all other interior vertices have 2. In total, there are $T-2$ degrees of freedom for moving the vertices while maintaining the combinatorial structure. If we consider the map sending any configuration to the T-tuple of signed areas, the image must satisfy two relations. One is that the sum of the areas is 1. What is the other?

Problem 10 (Ken Stephenson)**.** *Uniqueness of inversive distance packings.* Let K be a doubly periodic hexagonal lattice in the plane, that is, some affine image of a regular hexagonal lattice. Define a circle packing P for K by centering a circle of radius r at every lattice point, where r is sufficiently small that no two circles intersect. For each pair of neighboring lattice points record the inversive distance between their circles. (The Möbius invariant *inversive distance* between separated circles $C_1 = C(z, s)$ and $C_2 = C(w, t)$ is given by $(C_1, C_2) = |s^2+t^2-|z-w|^2|/2st$. See [1, Appendix E] for details on inversive distance circle packings.)

By lattice periodicity, just three inversive distances occur, $a, b, c \geq 1$, each associated with an axis direction for K: every pair of circles that are neighbors in the parallel direction share that inversive distance.

Question: Is the packing P rigid? That is, suppose Q is a second circle packing for K whose circles realize the corresponding inversive distances. Is it the case that all circles of Q share a common radius?

Dennis Sullivan [2] proved that the answer is yes when $a = b = c = 1$, that is, when every circle is tangent to its six neighbors. Zheng-Xu He [3] extended this to the case $a, b, c \in [0, 1]$, in which the circles overlap with specified overlap angles up to $\pi/2$.

[1] Ken Stephenson, *Introduction to Circle Packing: the Theory of Discrete Analytic Functions*, Cambridge Univ. Press (2005).

[2] Dennis Sullivan, *On the ergodic theory at infinity of an arbitrary discrete group of hyperbolic motions*, in: Riemann surfaces and related topics: Proceedings of the 1978 Stony Brook Conference, Ann. of Math. Stud. **97** (1981), 465–496.

[3] Zheng-Xu He, *Rigidity of infinite disk patterns*, Annals of Mathematics **32** (1999), 1–33.

Problem 11 (John Sullivan)**.** It has recently been shown [1] that any combinatorial triangulation of a two-torus (as a simplicial complex) can be realized geometrically in $\mathbb{R}^3$ (that is, embedded with flat triangles).

Any topological embedding of a torus in space (up to isotopy) determines not only the knot type (of the core curve) but also a marking of the torus, that is, a choice of complementary homology classes to be the meridian and longitude.

In which isotopy classes can a given combinatorial triangulation be realized? It is not hard, for instance, to show that the smallest triangulated torus (the Möbius torus) can only be realized as an unknot, and that the meridian and longitude must be chosen from the three homology classes that are realizable as edge cycles of length 3.

[1] Dan Archdeacon, C. Paul Bonnington and Joanna A. Ellis-Monaghan, *How to exhibit toroidal maps in space*, Discr. Comput. Geom. **38** (2007), 573–594.

Problem 12 (Feng Luo and Igor Pak)**.** Given a simplicial convex 3-polytope, is it infinitesimally rigid when at each edge either length *or* dihedral angle is fixed and at least one edge length is given?

Dehn's infinitesimal rigidity says the answer is yes if each edge length is given. Also the recent work of A. Pogorelov [1] shows infinitesimal rigidity up to scaling when dihedral angles at all edges are fixed, assuming all face angles are acute. Most recently, R. Mazzeo announced a complete solution of the Stoker conjecture, thus in particular removing the acute angle condition. This question of mixed type is motivated by the variational principle point of view. For instance, it is now known that a circle packing metric on a triangulated surface is determined when at each vertex either the curvature or the radius is given. On the other hand, *global* rigidity is not always true.

[1] Pogorelov, A. V.: *On a problem of Stoker* (Russian), Dokl. Akad. Nauk, Ross. Akad. Nauk **385** (2002), no. 1, 25–27; English translation in Dokl. Math. **66** (2002), no. 1, 19–21.

Problem 13 (Joseph O'Rourke)**.** Given a simple piecewise-geodesic curve on S^2, develop it onto the plane (same lengths and angles). Find conditions which guarantee that the developed image does not intersect itself. This is true if we start with a closed convex polygon on S^2. What about star-shaped polygons?

Problem 14 (Alexander Bobenko)**.** Are there (discrete) integrable systems in dimension four and higher? An n-dimensional discrete system is an equation for a function (field) defined at the vertices of an n-dimensional cube. Given values of the function at all the vertices of the cube but one, the discrete system determines the value at the last vertex. Following [1], a discrete system is called integrable if it is consistent, i. e., can be consistently set at all n-dimensional faces of an $(n+1)$-dimensional cube. The same problem can be also formulated for the systems with the fields on edges or faces. Many incidence relations in discrete differential geometry are discrete integrable systems.

There are many 2-dimensional and a few 3-dimensional discrete integrable systems (see the talk of Suris in this workshop). No examples in dimension four and higher are known.

[1] Alexander I. Bobenko, Yuri B. Suris, *Discrete Differential Geometry: Integrable Structure*, Graduate Studies in Mathematics, Vol. 98, AMS, 2008.

Lattice triangulations of 3-space and of the 3-torus

Ulrich Brehm
(joint work with Wolfgang Kühnel)

Parallelohedra (i.e., convex bodies which tile by translation) are a very classical and important topic in crystallography and in the theory of tilings. Already Voronoi showed that there are exactly five types of 3-dimensional parallelohedra [2]. Of particular interest are primitive tilings of $\mathbb{R}^d$, i.e., tilings where exactly $d+1$ tiles meet in every vertex. Dually one gets triangulations of $\mathbb{R}^d$, where a group $\Gamma \cong \mathbb{Z}^d$ of translations operates transitively on the set of vertices.

In the 3-dimensional case exactly one of the five types of parallelohedra is the prototile for a primitive tiling. It is the truncated octahedron (with 14 facets).

If one drops the assumption of "convexity of the tiles," the situation changes drastically and one gets already in the 3-dimensional case infinitely many types of primitive lattice tilings by "nonconvex parallelohedra". We prefer the dual point of view and consider triangulations by "curvilinear simplices". A more systematic investigation of such "lattice triangulations" is the topic of the talk. We start with the basic definitions.

Definitions. An *abstract lattice triangulation* of $\mathbb{R}^d$ is a pair $(\mathcal{K}, G)$, where $\mathcal{K}$ is an infinite simplicial complex with $|\mathcal{K}| \cong \mathbb{R}^d$ and $G \cong \mathbb{Z}^d$ is a group of automorphisms of $\mathcal{K}$ acting transitively on the set of vertices.

Let $\Gamma \subseteq \mathbb{R}^d, \Gamma \cong \mathbb{Z}^d$ be a lattice. If there exists a homeomorphism $\varphi : |\mathcal{K}| \to \mathbb{R}^d$ and a group isomorphism $\alpha : G \to \Gamma$, such that for all $g \in G$ and $x \in |\mathcal{K}|$ the equality $\varphi(g(x)) = \varphi(x) + \alpha(g)$ holds, we call $(\mathcal{K}, G)$ *geometrically realizable* and the induced tiling of $\mathbb{R}^d$ a *lattice triangulation* (with lattice Γ).

Two abstract lattice triangulations $(\mathcal{K}, G)$ and $(\mathcal{K}', G')$ are *isomorphic* if there exists a simplicial isomorphism $f : \mathcal{K} \to \mathcal{K}'$ and a group isomorphism $\alpha : G \to G'$ such that $f(g(x)) = \alpha(g)(f(x))$ for all $g \in G$ and vertices $x \in |\mathcal{K}|$.

Two lattice triangulations are called *equivalent* if their underlying abstract lattice triangulations $(\mathcal{K}, G)$ and $(\mathcal{K}', G')$, respectively, are isomorphic. For an abstract lattice triangulation we can assume w.l.o.g. that the set of vertices is $\mathbb{Z}^d$ and $G = \mathbb{Z}^d$ operating by addition. Then we define the *basic link* $\mathcal{L}$ as the link of 0.

Proposition 1. *$\mathcal{L}$ has the following properties:*
(1) *$\mathcal{L}$ is a simplicial S^{d-1} with vertices in $\mathbb{Z}^d \setminus \{0\}$*
(2) *$\langle x_1, \cdots, x_d \rangle \in \mathcal{L} \Rightarrow \langle -x_1, x_2 - x_1, \cdots, x_d - x_1 \rangle \in \mathcal{L}$*
(3) *The set of vertices of $\mathcal{L}$ generates $\mathbb{Z}^d$.*

Definition. If $\mathcal{L}$ is a simplicial S^{d-1} satisfying (1), (2), (3), it is called an *abstract basic link*.

Proposition 2. *If $\mathcal{L}$ is an abstract basic link then there is a unique $\mathbb{Z}^d$-invariant simplicial complex $\mathcal{K}$ having $\mathcal{L}$ as its basic link.*

Proposition 3. *Two $\mathbb{Z}^d$-invariant abstract lattice triangulations are equivalent if and only if there is a $\varphi \in GL(d,\mathbb{Z})$ such that its restriction to the vertex set of the basic links $\mathcal{L}$, $\mathcal{L}'$ is a simplicial isomorphism.*

In the remaining part of the talk we consider in more detail the 3-dimensional case, although we are aware that most of the constructions and ideas can be generalized to the d-dimensional case.

The basic construction method is a simultaneous application of bistellar flips. Let $\mathcal{L}$ be an abstract basic link and $\langle x,y,z\rangle \in \mathcal{L}$. Then there is a unique $u \in \mathbb{Z}^3\backslash\{0\}$ with $\langle x-u, y-u, z-u\rangle \in \mathcal{L}$. If u is not a vertex of $\mathcal{L}$ then simultaneous bistellar flips can be applied yielding another abstract link $\mathcal{L}'$ with u and $-u$ as additional vertices and eight triangles being replaced by twelve other triangles. This is our basic operation. If $\mathcal{L}'$ is an abstract link with a 3-valent vertex u then the inverse operation can be applied.

Proposition 4. *Geometric realizability is preserved under the operation described above and under its inverse.*

Starting with the basic link of the unique standard lattice triangulation with ordinary tetrahedra we get explicitly infinitely many geometrically realizable lattice triangulations of $\mathbb{R}^3$. Some of these are investigated in more detail. Particularly remarkable is a basic link with 18 vertices having an automorphism group of order 24 and without 3-valent vertices.

Theorem 1. *For each even $n \geq 14$ there is a lattice triangulation of $\mathbb{R}^3$ for which the basic link has n vertices.*

Factorizing a lattice triangulation of $\mathbb{R}^3$ by a suitable subgroup of the lattice Γ one gets a simplicial 3-torus.

Proposition 5. *Let $\mathcal{L}$ be an abstract basic link and $f : \mathbb{Z}^3 \to G$ be a surjective group homomorphism such that f is injective on the union of $\{0\}$ and the set of vertices of $\mathcal{L}$. Then $\{\langle a, f(x)+a, f(y)+a, f(z)+a\rangle | \langle x,y,z\rangle \in \mathcal{L}, a \in G\}$ is the set of tetrahedra of a simplicial 3-torus with a vertex transitive group G of automorphisms.*

Theorem 2. *For each odd $n \geq 15$ there is a neighbourly triangulation (i.e., any two vertices are joined by an edge) of the 3-torus with n vertices and Z_n as a group of automorphisms. Moreover each of these tori has a geometrically realizable lattice triangulation as universal covering.*

References

[1] U. Brehm and W. Kühnel, Lattice triangulations of $\mathbb{E}^3$ and of the 3-torus. Preprint 2008.

[2] M. G. Voronoi, *Nouvelles applications des paramètres continus à la théorie des formes quadratiques – Deuxième Mémoire. Recherches sur les parallélloèdres primitifs.* J. Reine Angew. Math. **134** (1908), 198–287, ibid. **136** (1909), 67–181.

Lattice triangulations of 3-space, and PL curvature

Wolfgang Kühnel
(joint work with Ulrich Brehm)

We consider *lattice triangulations* – abstract and geometric in Euclidean space – as defined in the talk by Ulrich Brehm. Usually the PL curvature of a combinatorial 3-manifold, equipped with a simplexwise Euclidean metric (or discrete metric or PL metric), is defined as follows: For any edge e let β_i denote the interior dihedral angles at e. Then the quantity

$$K(e) := 2\pi - \sum_i \beta_i$$

is called the *PL curvature* along e. In a triangulation of flat Euclidean space we have $K \equiv 0$ provided that all simplices are Euclidean. This is to be understood in the sense that a Euclidean d-dimensional simplex is assumed to be isometric with the convex hull of $d+1$ points in Euclidean d-space which are in general position. In particular all edges have to be straight in this case. In contrast, a topological simplex is assumed to be only homeomorphic with a Euclidean simplex, possibly with curved edges. Degenerate simplices with volume zero are not admitted here. In Riemannian geometry the following is certainly a trivial statement:

Proposition (trivial)**.** *The unique flat metric on the Euclidean d-space is G-equivariant for any lattice $G \cong \mathbb{Z}^d$ acting by pure translations, meaning that G acts by isometries.*

The question is whether this carries over to the discrete case.

Question: *Assume that we have an abstract lattice triangulation of d-space where a group $G \cong \mathbb{Z}^d$ acts transitively on the set of vertices, and where any simplex is isometric with a Euclidean simplex (i.e., we have an associated PL metric). Is it true that on the same triangulation we can associate a flat PL metric, still preserving the G-equivariance and the property of the simplices to be Euclidean?*

It turns out that the answer is "yes" only in dimension $d = 2$ and "no" in any dimension $d \geq 3$. In 3-space a particular family of examples can be described as the universal covering of certain triangulations of the 3-dimensional torus, see the talk by Ulrich Brehm.

Theorem 1. *Assume we have an abstract lattice triangulation of Euclidean 3-space, equipped with a PL metric by Euclidean simplices such that the group $G \cong \mathbb{Z}^3$ of all translations of the lattice acts isometrically with respect to this PL metric. Assume further that the PL curvature $K(e)$ vanishes along all edges e. Then the triangulation is combinatorially unique and, moreover, the metric is affinely equivalent with the one of the standard lattice triangulation of 3-space. This standard triangulation is the dual of the tiling by translates of the truncated octahedron (also called orthic tetrakaidecahedron* [3]*).*

Each vertex link in the unique standard lattice triangulation is combinatorially equivalent to a subdivided cube with 14 vertices (one extra vertex at the centre of each of the six squares of the cube). Geometrically, the vertex link can also be regarded as a subdivided rhombidodecahedron where each rhombus is divided into two triangles by using the short diagonal. For a picture see [4].

The proof of Theorem 1 is done in the following three steps:

(1) From the condition $K(e) = 0$ at the edges we conclude that a neighborhood of each vertex is isometric with Euclidean 3-space. One just has to consider the distance sphere from the vertex with a certain small radius. We remark that this step breaks down for $d = 2$ because the distance sphere there admits coverings onto itself.

(2) It follows that the flat Euclidean space is triangulated by Euclidean tetrahedra, and that the Euclidean group acts on it by translations and transitively on the vertices. Consequently, the dual of it is a primitive lattice tiling of Euclidean 3-space. *Primitive* means that at any vertex precisely four tetrahedra meet, the minimum number.

(3) By a classical theorem of Fedorov-Voronoi [6] there is precisely one primitive lattice tiling of 3-space (up to affine transformations), namely, the one where the prototile is a truncated octahedron. An alternative direct proof for the uniqueness of the lattice triangulation in 3-space (without the duality argument) see [2].

On the other hand we have the following result (see the talk by Ulrich Brehm):

Theorem 2. *There are infinitely many combinatorially distinct non-standard lattice triangulations of Euclidean 3-space. For them no associated $\mathbb{Z}^3$-equivariant PL metric can be flat. However, the flat metric becomes equivariant if we realize the tetrahedra as topological tetrahedra. The vertex link can have an arbitrarily large even number of vertices.*

This proves that the answer to the question above is "no" for $d = 3$. At least in some cases it will be possible to realize a flat metric with Euclidean tetrahedra on the same triangulation, if the lattice symmetry is broken.

The uniqueness of a primitive lattice tiling fails to hold in any dimension $d \geq 4$. There are three distinct items for $d = 4$, as already classified by Voronoi [6]. However, in any dimension $d \geq 2$ there is a standard lattice triangulation of d-space, just given by the standard triangulation of each cube in the cubical tiling. Furthermore, this admits a quotient by a sublattice which is a combinatorial d-torus. This works for any number $n \geq 2^{d+1} - 1$ of vertices [4], [5] and with $\mathbb{Z}_n$-symmetry on the 3-torus. Here only the case $n = 2^{d+1} - 1$ leads to a *neighborly* triangulation meaning that any two vertices are joined by an edge. The question is whether there are similar neighborly triangulations of the 3-torus with unbounded number $n \geq 15$ of vertices (and with a vertex transitive $\mathbb{Z}_n$-symmetry). We recall a result from the talk by Ulrich Brehm and add a consequence regarding the PL curvature.

Theorem 3. *The Euclidean* 3*-space admits infinitely many* G*-equivariant triangulation by topological simplices for the group* $G \cong \mathbb{Z}^3$ *of all translations of a lattice in such a way that the set of vertices coincides with that lattice. Each vertex link can have any even number* $n - 1 \geq 14$ *of vertices. There are neighborly* n*-vertex triangulations of the* 3*-torus as quotients admitting a transitive* $\mathbb{Z}_n$*-action by translations. Moreover, for all cases* $n \geq 17$ *it is not possible to associate a flat discrete metric to the triangulation such that the group* $\mathbb{Z}_n$ *acts by isometries.*

References

[1] U. Brehm and W. Kühnel, Lattice triangulations of $\mathbb{E}^3$ and of the 3-torus. Preprint 2008

[2] A.Grigis, *Triangulation du tore de dimension* 4. Geom. Dedicata **69** (1998), 121–139

[3] Lord Kelvin, *On homogeneous division of space*, Proc. Royal Soc. London **55** (1894), 1–9

[4] W.Kühnel & G.Lassmann, *The rhombidodecahedral tessellation of* 3*-space and a particular* 15*-vertex triangulation of the* 3*-dimensional torus.* Manuscripta Math. **49** (1984), 51–77

[5] W.Kühnel & G.Lassmann, *Combinatorial d-tori with a large symmetry group.* Discrete Comput. Geom. **3** (1988), 169–176

[6] M.G.Voronoi, *Nouvelles applications des paramètres continus à la théorie des formes quadratiques – Deuxième Mémoire. Recherches sur les parallélloèdres primitifs.* J. Reine Angew. Math. **134** (1908), 198–287, ibid. **136** (1909), 67–181.

Symmetry as a sufficient condition for a finite flex

Bernd Schulze

A d-dimensional framework is a pair (G, p), where G is a graph and p is a map that assigns to each vertex of G a point in Euclidean d-space. We can think of a framework as a collection of rigid bars (corresponding to the edges of G) connected together at their ends by flexible joints (corresponding to the vertices of G) which allow bending in any direction. This talk is concerned with the detection of finite flexes of symmetric frameworks, i.e., flexes that move the joints of a framework on differentiable displacement paths while holding the lengths of all bars fixed and changing the distance between two unconnected joints.

It is well known that if a framework (G, p) has a finite flex, then it also has an infinitesimal flex, i.e., an assignment of velocity vectors, one to each joint, that neither stretch nor compress the bars of (G, p) [3, 4]. In 1978 L. Asimov and B. Roth showed that for 'generic' frameworks the existence of an infinitesimal flex also implies the existence of a finite flex [1]. This result, however, is in general not applicable to frameworks that possess non-trivial symmetries, because the joints of a symmetric framework are typically forced into non-generic positions.

In this talk we present some new results that provide sufficient conditions for the existence of a finite flex of a symmetric framework. In particular, we show that if the joints of a symmetric framework (G, p) are positioned as 'generically' as possible (subject to the given symmetry conditions) and there exists a 'fully-symmetric' infinitesimal flex of (G, p) (i.e., the velocity vectors of the infinitesimal flex remain unaltered under all symmetry operations of (G, p)), then (G, p) also possesses a 'symmetry-preserving' finite flex, i.e., a flex which displaces the joints of

(G, p) in such a way that all the resulting frameworks have the same symmetry as (G, p) (or possibly higher symmetry). This and other related results are obtained by symmetrizing techniques described by L. Asimov and B. Roth in [1] and by using the fact that the rigidity matrix of a symmetric framework can be transformed into a block-diagonalized form by means of group representation theory techniques [2].

References

[1] L. Asimov and B. Roth, *The Rigidity Of Graphs*, Trans. Amer. Math. Soc. **245** (1978), 279–289.

[2] B. Schulze, *Block-diagonalized rigidity matrices of symmetric frameworks and applications*, in preparation, York University, Toronto, Canada (2009).

[3] W. Whiteley, *Some matroids from Discrete Applied Geometry*, Contemp. Math. **197** (1996), 171–311.

[4] W. Whiteley, *Rigidity and Scene Analysis*, Handbook of Discrete and Computational Geometry, Goodman, J.E., O'Rourke J., editors, Chapman & Hall/CRC (2006), 1327–1354.

Persistence simplification of discrete Morse functions on surfaces

Ulrich Bauer

(joint work with Carsten Lange and Max Wardetzky)

1. Introduction

We apply the concept of persistent homology [1] to Forman's discrete Morse theory [2] on regular 2-manifold CW complexes and solve the problem of minimizing the number of critical points among all functions within a prescribed distance δ from a given input function. Our result achieves a lower bound on the number of critical points and improves on previous work [3] by a factor of two.

2. Discrete Morse theory

Let $\mathcal{K}$ be a finite CW complex and K the set of cells of $\mathcal{K}$. The cell σ is a *face* of τ, denoted by $\sigma < \tau$, if σ is in the boundary of τ. *Facets* are faces of codimension 1. If the attaching maps are homeomorphisms, $\mathcal{K}$ is called a *regular* complex. A *combinatorial surface* is a regular CW complex whose underlying space is a 2-manifold.

Discrete vector fields are one of the central concepts of discrete Morse theory. They are a purely combinatorial analogon of classical vector fields.

Definition (Discrete vector field)**.** A *discrete vector field* V on a regular CW complex $\mathcal{K}$ is a set of pairs of cells $(\sigma, \tau) \in K \times K$, with σ a facet of τ, such that each cell of K is contained in at most one pair of V.

Definition (V-path)**.** Let V be a discrete vector field. A V-path Γ from a cell σ_0 to a cell σ_r is a sequence $\sigma_0\tau_0\sigma_1 \dots \tau_{r-1}\sigma_r$ of cells such that for every $0 \le i \le r-1$:

$$\sigma_i \text{ is a facet of } \tau_i \quad \text{and} \quad (\sigma_i, \tau_i) \in V,$$
$$\sigma_{i+1} \text{ is a facet of } \tau_i \quad \text{and} \quad (\sigma_{i+1}, \tau_i) \notin V.$$

A V-path is a *nontrivial closed path* if $\sigma_0 = \sigma_r$ and $r > 0$.

Definition (Discrete gradient vector field)**.** A *gradient vector field* is a discrete vector field V that does not admit any nontrivial closed V-paths.

Definition (Critical cell)**.** A cell σ is a *critical cell* with respect to a discrete gradient vector field V if σ is not contained in any pair of V. A cell that is not critical is a *regular cell*.

The main technique for reducing the number of critical points is that of *reversing* a gradient vector field V along a V-path between two critical cells τ and σ:

Theorem ([2], Theorem 11.1)**.** *Let σ and τ be critical cells of a gradient vector field V with a unique V-path Γ from $\partial\tau$ to σ. Then there is a gradient vector field $\widetilde{V}$ obtained by reversing V along the path Γ. The critial cells of $\widetilde{V}$ are exactly the critical cells of V other than $\{\sigma, \tau\}$. In particular, $V = \widetilde{V}$ except along the path Γ.*

As in smooth Morse theory, a discrete gradient vector field can be understood as the gradient of some function in the following sense:

Definition ((Pseudo-)Morse function)**.** A *discrete Morse function* is a function $f : K \to \mathbb{R}$ on the cells of a regular CW complex $\mathcal{K}$ if there is a gradient vector field V such that for all pairs of cells we have

$$\sigma \text{ is a facet of } \tau \Rightarrow \begin{cases} f(\sigma) < f(\tau) & \text{if } (\sigma, \tau) \notin V, \\ f(\sigma) \geq f(\tau) & \text{if } (\sigma, \tau) \in V. \end{cases}$$

For a *discrete pseudo-Morse function*, the strict inequality is replaced by a weak one, i.e., $f(\sigma) \leq f(\tau)$ if $(\sigma, \tau) \notin V$. In either case, we call V *consistent with* f.

Definition (Induced partial order)**.** The partial order $\prec_V$ *induced* by a discrete gradient vector field V is the transitive relation generated by

$$\sigma \text{ is a facet of } \tau \Rightarrow \begin{cases} \sigma \prec_V \tau & \text{if } (\sigma, \tau) \notin V, \\ \sigma \succ_V \tau & \text{if } (\sigma, \tau) \in V. \end{cases}$$

For any pseudo-Morse function g consistent with V and any pair of cells (ϕ, ρ), $\phi \prec_V \rho$ implies $g(\phi) \leq g(\rho)$.

3. Persistent Morse homology

Homological persistence [1] is used to investigate the change of the homology groups in a sequence of nested topological spaces. We study nested subcomplexes of a given CW complex.

Definition (Level subcomplex)**.** Let f be a discrete Morse function on a regular CW complex $\mathcal{K}$. For a cell $\sigma \in K$, the *level subcomplex* is the subcomplex of $\mathcal{K}$ consisting of all cells ρ with $f(\rho) \leq f(\sigma)$ together with their faces:

$$\mathcal{K}(\sigma) := \bigcup_{\substack{\rho \in K \\ f(\rho) \leq f(\sigma)}} \bigcup_{\substack{\phi \in K \\ \phi \leq \rho}} \phi \,.$$

For $\mathcal{K}(\phi) \subset \mathcal{K}(\rho)$, let $i_*^{\phi,\rho} : H_*(\mathcal{K}(\phi)) \to H_*(\mathcal{K}(\rho))$ denote the homomorphism induced by inclusion. Let σ and τ be critical cells of dimension d and $(d+1)$, respectively, such that $f(\sigma) < f(\tau)$. The *predecessor* of σ is the cell σ_- with the largest f-value such that $f(\sigma_-) < f(\sigma)$, and similarly for τ_-. Now consider the sequence

$$H_d(\mathcal{K}(\sigma_-)) \to H_d(\mathcal{K}(\sigma)) \to H_d(\mathcal{K}(\tau_-)) \to H_d(\mathcal{K}(\tau))$$

induced by inclusion.

Definition (Birth, death, persistence pair)**.** Let f be an injective Morse function on a regular CW complex. We say that a class $h \in H_*(\mathcal{K}(\sigma))$ is *born at* (or *created by*) σ if

$$h \notin \operatorname{im}(i_*^{\sigma-,\sigma}).$$

Moreover, we say that a class $h \in H_*(\mathcal{K}(\sigma))$ that is born at σ *dies entering* (or gets *merged by*) τ if

$$i_d^{\sigma,\tau}(h) \in \operatorname{im}(i_*^{\sigma-,\tau}) \quad \text{but} \quad i_d^{\sigma,\tau-}(h) \notin \operatorname{im}(i_*^{\sigma-,\tau-}).$$

If there exists a class h that is born at σ and dies entering τ, then (σ,τ) is a *persistence pair*. The difference $f(\tau) - f(\sigma)$ is called the *persistence* of (σ,τ).

To uniquely define persistence pairs for a *pseudo-Morse* function f consistent with some gradient vector field V, we require a total order on the cells. This can be achieved by extending the partial order $\prec_V$ to a total order, which allows us to speak about persistence pairs of (f,V).

4. Topological simplification of functions

From now on, let f be a pseudo-Morse function consistent with a discrete gradient vector field V on a combinatorial surface $\mathcal{K}$. From the stability theorem for persistence diagrams [4], we can deduce the following lower bound on the number of persistence pairs, and therefore on the number of critical points:

Lemma. *For a pseudo-Morse function f_δ with $\|f_\delta - f\|_\infty < \delta$ and consistent with a gradient vector field V_δ, the number of persistence pairs of (f_δ, V_δ) is bounded from below by the number of persistence pairs of f with persistence $\geq 2\delta$.*

We are interested in functions that achieve this lower bound:

Definition (Perfect δ-simplification)**.** A *perfect δ-simplification* of (f,V) is a pseudo-Morse function f_δ consistent with a gradient vector field V_δ, such that $\|f_\delta - f\|_\infty < \delta$ and the number of persistence pairs of (f_δ, V_δ) is equal to the number of persistence pairs of f with persistence $\geq 2\delta$.

Our main result states that a perfect δ-simplification always exists for a discrete pseudo-Morse function on a combinatorial surface.

Theorem. *Let f be a discrete pseudo-Morse function on a combinatorial surface. Then there exists a perfect δ-simplification of f.*

The proof of this theorem is constructive. An analogous statement is not true in higher dimensions or for non-manifold complexes.

References

[1] H. Edelsbrunner, D. Letscher, and A. Zomorodian. Topological persistence and simplification. *Discrete Comput. Geom.*, 28(4):511–533, 2002.
[2] R. Forman. Morse theory for cell complexes. *Adv. Math.*, 134(1):90–145, 1998.
[3] H. Edelsbrunner, D. Morozov, and V. Pascucci. Persistence-sensitive simplification of functions on 2-manifolds. In *SCG '06: Proceedings of the 22nd ACM Symposium on Computational Geometry*, pages 127–134. ACM, 2006.
[4] D. Cohen-Steiner, H. Edelsbrunner, and J. Harer. Stability of persistence diagrams. *Discrete Comput. Geom.*, 37(1):103–120, 2007.

Approximation of conformal mappings by circle patterns

Ulrike Bücking

Conformal mappings constitute an important class in the field of complex analysis. They may be characterized by the fact that infinitesimal circles are mapped to infinitesimal circles. Thurston first introduced in his talk [10] the idea to use finite circles, in particular circle packings, to define a discrete conformal mapping. Remember that an *embedded planar circle packing* is a configuration of closed disks with disjoint interiors in the plane $\mathbb{C}$. Various connections between circle packings and classical complex analysis have already been studied. A beautiful introduction and surway is presented by Stephenson in [9].

The class of *circle patterns* generalizes circle packings as for each circle packing there is an associated orthogonal circle pattern. Simply add a circle for each triangular face which passes through the three touching points. To define a circle pattern we use a planar graph as combinatorial data. The circles correspond to vertices and the edges specify which circles should intersect. The intersection angles are given using a labelling on the edges. Thus an edge corresponds to a kite of two intersecting circles as in Figure 1. A face of the graph corresponds to a point where all the circles corresponding to the incident vertices intersect. Such intersection points are colored black in Figure 1. Moreover, for interior vertices the kites corresponding to the incident edges have disjoint interiors and their union is homeomorphic to a closed disk. Thus to a circle pattern we also associate a kite pattern.

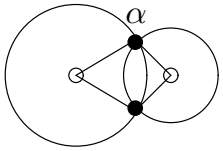

Figure 1. The exterior intersection angle α of two intersecting circles and the associated kite built from centers and intersection points.

Given two circle patterns $\mathscr{C}_1$ and $\mathscr{C}_2$ with the same combinatorics and intersection angles, define a mapping $g_{\mathscr{C}} : \mathscr{C}_1 \to \mathscr{C}_2$. Namely, take $g_{\mathscr{C}}$ to map the centers of circles and the intersection points of $\mathscr{C}_1$ corresponding to vertices and faces of G to the corresponding centers of circles and intersection points of $\mathscr{C}_2$ and extend it to an affine map on each kite.

For a given conformal map g we use an analytic approach and specify suitable boundary values for the radius function according to $|g'|$ in order to define the (approximating) mappings $g_{\mathscr{C}}$. Generalizing ideas of Schramm's convergence proof in [8] we obtain convergence in C^1 on compact sets if we take for $\mathscr{C}_1$ a sequence of isoradial circle patterns (i.e., all radii are equal) with decreasing radii $\varepsilon \to 0$ which approximate the domain of g. Note in particular that the combinatorics of the circle patterns $\mathscr{C}_1$ may be irregular or change within the sequence. More precisely, we obtain for example the following result.

Theorem. *Let $W \subset \mathbb{C}$ be open and let $g : W \to \mathbb{C}$ be a locally injective holomorphic function. Let $K \subset \mathbb{C}$ be a compact set whose interior is simply connected and which is contained in W.*

Consider a sequence $\mathscr{C}_1^{(n)}$ of isoradial circle patterns with decreasing radii $\varepsilon_n \to 0$. Assume that the region covered by the closed disks filling the circles of the circle pattern $\mathscr{C}_1^{(n)}$ is contained in W and covers K for each $n \in \mathbb{N}$. Furthermore, the centers of circles not contained in K have a distance of at most $2\varepsilon_n$ to K. Assume further that the intersection angles of the circle patterns $\mathscr{C}_1^{(n)}$ are uniformly bounded away from 0 and π.

Then a sequence of image circle patterns $\mathscr{C}_2^{(n)}$ can be defined by setting $r_n(v) = \varepsilon_n |g'(v)|$ for the radius $r_n(v)$ of the boundary centers of circles, where v is the corresponding center of circle of $\mathscr{C}_1^{(n)}$. Furthermore, we adjust the translational and rotational freedom of $\mathscr{C}_2^{(n)}$ according to the image of g at one vertex (per connected component of the circle pattern). Then we have for all centers of circles w of $\mathscr{C}_1^{(n)}$

$$g(w) = g_{\mathscr{C}^{(n)}}(w) + \mathcal{O}(\varepsilon_n) \tag{1}$$

$$|g'(w)| = r_n(w)/\varepsilon_n + \mathcal{O}(\varepsilon_n). \tag{2}$$

The implicit constants in $\mathcal{O}(\dots)$ of these estimations depend on g and W, K, and the uniform bound on the intersection angles, but not on the combinatorics of $\mathscr{C}_1^{(n)}$.

The main idea of the proof is to consider a "nonlinear discrete Laplace equation" for the radius function r_n. This equation turns out to be a (good) approximation of a known linear Laplace equation and can be used in the case of isoradial circle patterns $\mathscr{C}_1^{(n)}$ to compare discrete and smooth solutions of the corresponding elliptic problems. In particular, we obtain (2) if ε_n is small enough.

Isoradial circle patterns are closely related to rhombic embeddings. Simply bicolor the vertices of such an embedding and add circles centered at all white (or all black) vertices with radius equal to the edge length. For rhombic embeddings,

there is an asymptotic development given by Kenyon in [7] of a discrete Green's function which is slightly generalized in [2] and in [4]. Using similar ideas as Duffin in [5], we can generalize theorems of discrete potential theory concerning the regularity of solutions of a discrete Laplace equation, see [2]. This regularity lemma, estimation (2), and a Taylor expansion of the analytic closing condition for the radii form the basis of our proof of C^1-convergence claimed in the theorem.The proof generalizes a method used by He and Schramm in [6].

Using a repeated application of the regularity lemma, we also obtain C^∞-convergence on compact sets for a class of isoradial circle patterns. In order to define higher derivatives, we consider the rhombic embeddings as combinatorial surfaces in $\mathbb{Z}^{d_n}$ for appropriate d_n as in [1]. Using flips of 3-dimensional cubes, this original surfaces can be changed without changing their boundary curve. This leads to some region reached by flips in $\mathbb{Z}^{d_n}$. Here we still have the same estimations. For a fixed copamct subset K we now additionally assume that the combinatorial distance in at least two directions of this region is comparable to the combinatorial distance to the boundary, independently of n.

An extended and more detailed version of partially weaker results can be found in [3, 2].

References

[1] Alexander I. Bobenko, Christian Mercat, and Yuri B. Suris, *Linear and nonlinear theories of discrete analytic functions. Integrable structure and isomonodromic Green's function*, J. reine angew. Math. **583** (2005), pp. 117–161.

[2] Ulrike Bücking, *Approximation of conformal mappings by circle patterns.* Geom. Dedicata **137**, 163–197 (2008)

[3] Ulrike Bücking, Approximation of conformal mappings by circle patterns and discrete minimal surfaces. Ph.D. thesis, Technische Universität Berlin (2007). Published online at http://opus.kobv.de/tuberlin/volltexte/2008/1764/

[4] Dmitry Chelkak and Stanislav Smirnov, *Discrete complex analysis on isoradial graphs.* arXiv:0810.2188v1 [math.CV] (2008)

[5] Richard J. Duffin, *Discrete potential theory.* Duke Math. J. **20**, 233–251 (1953)

[6] Zheng-Xu He and Oded Schramm, *The C^∞-convergence of hexagonal disk packings to the Riemann map.* Acta Math. **180**, 219–245 (1998)

[7] Richard Kenyon, *The Laplacian and Dirac operators on critical planar graphs.* Invent. Math. **150**, 409–439 (2002)

[8] Oded Schramm, *Circle patterns with the combinatorics of the square grid.* Duke Math. J. **86**, 347–389 (1997)

[9] Kenneth Stephenson, Introduction to circle packing: the theory of discrete analytic functions. Cambridge University Press, New York (2005)

[10] William Thurston, The finite Riemann mapping theorem (1985). Invited address at the International Symposioum in Celebration of the proof of the Bieberbach Conjecture, Purdue University.

Stability of the fold

Herbert Edelsbrunner
(joint work with Dmitriy Morozov and Amit Patel)

The *fold* of a smooth mapping $f : \mathbb{M} \to \mathbb{R}^k$ from a compact n-manifold to Euclidean space of dimension $k \leq n$ is the image of the points at which the gradients of the k component functions are linearly dependent. The fold decomposes $\mathbb{R}^k$ into chambers which we glue along shared faces to form immersed k-manifolds. Measuring difference with the erosion distance (the Hausdorff distance for the complements adapted to immersed k-manifolds), we prove that the fold is stable. Specifically, for a second smooth mapping $g : \mathbb{M} \to \mathbb{R}^k$, we can form corresponding immersed k-manifolds such that the erosion distance between corresponding pairs is bounded from above by the maximum Euclidean distance between points $f(x)$ and $g(x)$.

References

[1] V. I. Arnol'd. *Catastrophe Theory.* Third edition, Springer-Verlag, Berlin, Germany, 1992.
[2] D. Cohen-Steiner, H. Edelsbrunner and J. Harer. Stability of persistence diagrams. *Discrete Comput. Geom.* **37** (2007), 103–120.
[3] H. Edelsbrunner, D. Morozov and A. Patel. Stability of the fold. Manuscript, Dept. Comput. Sci., Duke Univ., Durham, North Carolina, 2009.
[4] M. Golubitsky and V. Guillemin. *Stable Mappings and Their Singularities.* Springer-Verlag, New York, 1973.
[5] J. J. Koenderink. What does the occluding contour tell us about solid shape? *Perception* **13** (1984), 321–330.
[6] H. Whitney. On singularities of mappings of Euclidean space. I. Mappings of the plane to the plane. *Ann. Math.* **62** (1955), 374–410.

The Angle Defect and Its Generalizations

Ethan D. Bloch

The talk started with a review of what is most likely the first theorem in Discrete Differential Geometry, namely Descartes' Theorem concerning the angle defect for convex polyhedra in $\mathbb{R}^3$. This theorem was formulated before there was a subject called differential geometry. For a triangulated polyhedral surface M^2 in Euclidean space, the usual notion of curvature at a vertex v is the classical angle defect $d_v = 2\pi - \sum \alpha_i$, where the α_i are the angles of the triangles containing v. The classical angle defect satisfies some standard properties one would expect: it is invariant under polyhedral local isometries; it is locally defined; it is zero at a vertex that has a flat star; it is invariant under subdivision; and it satisfies the polyhedral Gauss-Bonnet Theorem, which says $\sum_v d_v = 2\pi\chi(M^2)$, where the summation is over all the vertices of M^2, and $\chi(M^2)$ is the Euler characteristic of M^2. Descartes' Theorem, which predates Euler, is the special case of the polyhedral Gauss-Bonnet Theorem when M^2 is a convex polyhedron in $\mathbb{R}^3$. See [8] for the text of Descartes' work on polyhedra, though Descartes did not give a proof of his theorem; see [12,

Chapter 25] for two proofs, the second of which is plausibly the one Descartes had in mind.

The bulk of the talk was a description of three methods for generalizing the classical angle defect to arbitrary finite simplicial complexes of all dimensions immersed in Euclidean space. One method, which I refer to as standard curvature, has been studied from a differential geometric point of view, for example in [1], [6] and [14]. This approach to generalizing the angle defect, which is based on exterior angles, is simple to define (though it does not directly resemble the classical angle defect), and its convergence properties have been well studied. On the other hand, the definition of standard curvature concentrates all the curvature at the vertices of simplicial comlexes, which does not necessarily correspond to our intuition about curvature in dimension greater than 2.

A different approach to generalizing the classical angle defect, known simply as the angle defect (or angle deficiency), has been studied in the case of convex polytopes by a number of combinatorialists, for example [13] and [9]. In [10] a Gauss-Bonnet theorem is proved for the angle defect in polytopes with underlying spaces that are manifolds. In contrast to standard curvature, the angle defect for convex polytopes is found at each cell of codimension at least 2, and the definition completely resembles the classical case.

The talk then discussed the possibility of extending the angle defect, as defined for polyhedral manifolds, to arbitrary finite immersed simplicial complexes. The definition of angle defect for polyhedral manifolds cannot be used without modification for arbitrary simplicial complexes, because it does not satisfy a Gauss-Bonnet theorem. A method of extending the angle defect to all finite immersed simplicial complexes, called the generalized angle defect, was then discussed, following [3]. This approach is based upon a simple topological decomposition of each simplicial complex, which allows for a suitable replacement for "2π" in the definition of the classical angle defect, where the replacement for a given simplex depends upon the topological nature of the neighborhood of the simplex. Both standard curvature and the generalized angle defect satisfy the expected properties, such as being locally defined, invariant under local isometries, and satisfying a Gauss-Bonnet theorem, though the Gauss-Bonnet Theorem for the generalized angle defect uses a modified Euler characteristic rather than the standard Euler characteristic; this modified Euler characteristic reduces to the standard Euler characteristic in the case of pseudomanifolds.

Although in many respects the generalized angle defect behaves as nicely as standard curvature, there is one exception. In [1, Section 5] it is stated that for an odd-dimensional polyhedral manifold, the standard curvature is zero at every vertex. It then follows from the Gauss-Bonnet theorem for standard curvature that every odd-dimensional polyhedral manifold has Euler characteristic zero (a well-known fact, but the method of [1, Section 5] yields a completely elementary proof). By contrast, the generalized angle defect is never zero for a convex polytope of any dimension, as seen in [13]. The talk then discussed the method of [4], where a variant of the generalized angle defect is defined that satisfies the nice properties

of the generalized angle defect, and yet also has the additional property that it is identically zero for any odd-dimensional simplicial complex K (of dimension at least 3) such that $\chi(\text{link}(\eta^i, K)) = 2$ for all i-simplices η^i of K, where i is an even integer such that $0 \leq i \leq n-1$. As a corollary, we deduce that if K is an odd-dimensional simplicial complex (of dimension at least 3) such that $\chi(\text{link}(\eta^i, K)) = 2$ for all i-simplices η^i of K, where i is an even integer such that $0 \leq i \leq n-1$, then K has Euler characteristic zero. This last result was proved for Euler spaces by different methods in [2], [7] and [11]; the result for Euler spaces turn out to be equivalent to the above corollary. The definition of this variant of the generalized angle defect is based, somewhat surprisingly, on a sequence that makes use of the Bernoulli numbers.

Given that there is more than one way to generalize the classical angle defect, it would be helpful to understand the relations between these generalizations, to determine which approach is useful in which situations. One method of comparing the different approaches would be to find an axiomatic characterization of each. Although the classical angle defect has been widely studied, there does not appear to be in the literature an axiomatic characterization of it. The final part of the talk discussed such a characterization in dimension 2, as found in [5], where it is proved that the classical angle defect for embedded simplicial surfaces is characterized by being invariant under simplicial isometries of stars and under subdivision, continuous, and satisfying the Gauss-Bonnet theorem with respect to the Euler characteristic. The same characterization also works for both standard curvature and the generalized angle defect for arbitrary immersed 2-dimensional simplicial complexes, except that for the generalized angle defect it is necessary to use the modified Euler characteristic.

References

[1] Thomas Banchoff, *Critical points and curvature for embedded polyhedra*, J. Differential Geom., **1**, (1967), 245–256.

[2] Thomas Banchoff, *Critical points and curvature for embedded polyhedra, II*, Progress in Math., **32**, (1983), 34–55.

[3] Ethan D. Bloch, *The angle defect for arbitrary polyhedra*, Beiträge Algebra Geom., **39**, (1998), 379–393.

[4] Ethan D. Bloch, *The angle defect for odd-dimensional simplicial manifolds*, Discrete Comput. Geom., **35**, (2006), 311–328.

[5] Ethan D. Bloch, *A characterization of the angle defect and the Euler characteristic in dimension* 2, to appear in Discrete Comput. Geom.

[6] Jeff Cheeger, Werner Müller, and Robert Schrader, *On the curvature of piecewise flat spaces*, Commun. Math. Phys., **92**, (1984), 405–454.

[7] Beifang Chen and Min Yan, *Eulerian* 2*-strata spaces*, J. Combin. Theory Ser. A, **85**, (1999), 1–28.

[8] Pasquale J. Federico, *Descartes on Polyhedra*, Springer-Verlag, New York, 1982.

[9] Branko Grünbaum, *Grassmann angles of convex polytopes*, Acta Math., **121**, (1968), 293–302.

[10] Branko Grünbaum and G. C. Shephard, *Descartes' theorem in n dimensions*, Enseign. Math. (2), **37**, (1991), 11–15.

[11] Colin MacLaurin and Guyan Robertson, *Euler Characteristic in Odd Dimensions*, Austral. Math. Soc. Gaz., **30**, (2003), 195–199.

[12] Igor Pak, Lectures on Discrete and Polyhedral Geometry, http://www.math.umn.edu/~pak/book.htm.
[13] G. C. Shephard, *Angle deficiencies of convex polytopes*, J. London Math. Soc., **43**, (1968), 325–336.
[14] M. Zähle, *Approximation and characterization of generalized Lipschitz-Killing curvatures*, Ann. Global Anal. Geom., **8**, (1990), 249–260.

Square pegs and beyond

Benjamin Matschke

This talk gave a collection of new theorems and re-opened conjectures related to the following famous square peg problem.

Conjecture (Square Peg Problem, Toeplitz [9]). *Does every continuously embedded circle in the plane contain four points spanning a square?*

This conjecture has been proved in the special case when the curves are smooth enough [7], [8], but it is still open for continuous curves. In particular, certain local spirals invalidate all known approaches for continuous curves, all of which use the fact that "generic" curves circumscribe an odd number of squares.

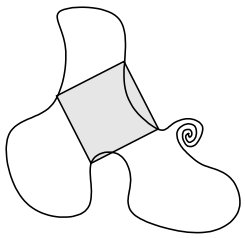

Equilateral Triangles on Curves

Theorem ([5, Thm. III.3.2]). *Let $d : S^1 \times S^1 \longrightarrow \mathbb{R}$ be a continuous symmetric map (a generalised metric). Then there are three points $x, y, z \in S^1$, not all of them equal, such that*

$$d(x, y) = d(x, z) = d(y, z).$$

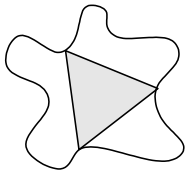

Polygons on Curves

Lemma ([5, Lem. III.4.7]). *Let $\gamma : S^1 \longrightarrow M$ be a C^∞-embedded curve in a Riemannian manifold M. Let n be a prime power ≥ 3, $\varepsilon > 0$ and let $P \subset (S^1)^n$ be the set of polygons whose vertices lie counter-clockwise on γ. Then there is a closed one-parameter family $S^1 \longrightarrow P$ of such polygons such that*

(1) each of the polygons are up to ε edge-regular, i. e. the edge ratios lie in the interval $[1 - \varepsilon, 1 + \varepsilon]$, and
(2) this one-parameter family is invariant under cyclic permutation of the vertices.

It can be proved using the fact that an isotopy of γ changes the solution set of all edge-regular n-gons on γ by a bordism. It turned out that Makeev already gave a very similar result [4, Thm. 3]. Here are two known and one new direct corollaries:

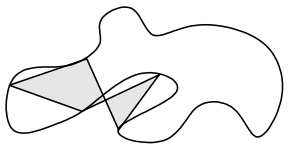

Corollary (Smooth Square Peg Problem, [7], [8]). *Each C^∞-embedded circle in the plane contains four points spanning a square.*

Corollary (A Conjecture of Hadwiger, [4, Thm. 4], [10, Thm. 11]). *Each knot, that is, a C^∞-embedded circle in $\mathbb{R}^3$, contains four points spanning a planar rhombus.*

Corollary (Blagojević–M., see [5, Thm. III.6.1]). *Let d_1 and d_2 be two symmetric distance functions on S^1, where d_1 is given by a C^∞-embedding of S^1 into a Riemannian manifold. Then there are three pairwise distinct points on S^1 forming an equilateral triangle with respect to d_1 and an isosceles triangle with respect to d_2.*

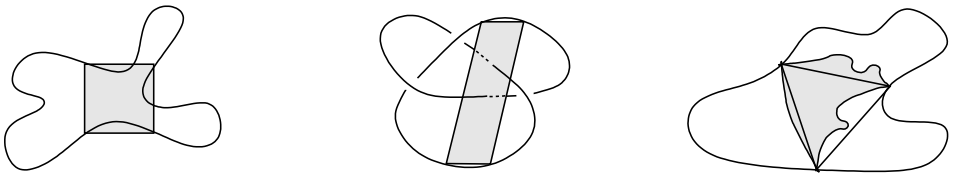

Rectangles on Curves

Conjecture. *Does every C^∞-embedded circle in $\mathbb{R}^2$ contain 4 points spanning a rectangle with prescribed edge-ratios?*

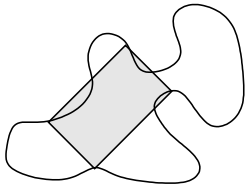

Griffiths [1] gave a proof of this conjecture, however there are slight errors in his calculation of orientations, such that an intersection number is zero instead of 16. Hence a desired intersection was not shown (that is, I do not know how to fix it [5, III.7]).

An ansatz towards solving this conjecture is the following: If the conjecture were wrong, then there would be a ratio $r > 0$ and a curve $\gamma : S^1 \to \mathbb{R}^2$ not containing rectangles of ratio r such that for all $\varepsilon > 0$ there is a $\mathbb{Z}_4$-invariant one-parameter family of up-to-ε-rectangles $S^1 \to (\gamma(S^1))^4$, such that the vertices of the rectangles lie counter-clockwise on γ [6]. It seems that this is essentially what topology can give us, but now more geometic ideas are needed to deduce a contradiction.

Tetrahedra on Closed Surfaces

Theorem ([5, Thm. III.8.5]). *Every smooth closed surface in $\mathbb{R}^3$ contains four points spanning a tetrahedron that is similar to a given one.*

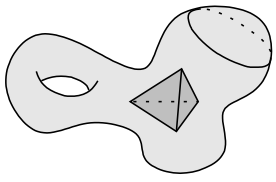

One can even prescribe an arbitrary vertex.

Regular Octahedra on Embedded Spheres

Conjecture. *Does every C^∞-embedded S^2 in $\mathbb{R}^3$ contain six points spanning a regular octahedron?*

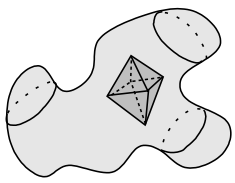

Guggenheimer [2] gave a proof of this conjecture, however there is an error in his main lemma, which he used to prove the smooth square peg problem, and which he claimed to be generalisable to prove the above conjecture.

This conjecture is probably very difficult and a solution would involve deeper geometric reasoning, since there is the following "topological counter-example". Let G be the symmetry group of the regular octahedron and $G_{or} \subset G$ the subgroup of orientation preserving symmetries. G acts on $(S^2)^6$ by permuting the coordinates in the same way as it permutes the vertices of the regular octahedron. Let G act on $\mathbb{R}^{12}$ by permuting the coordinates in the same way as it permutes the edges of the regular octahedron. The subrepresentation $(\mathbb{R} \cdot \mathbb{1})^{\perp} \subset \mathbb{R}^{12}$ is denoted by Y. Let

$$X := \{(x_1 \dots x_6) \in (S^2)^6 \mid x_i \text{ are pairwise distinct}\}.$$

Then any embedding $\Gamma : S^2 \to \mathbb{R}^3$ gives us a test map

$$t : (S^2)^6 \longrightarrow_G Y,$$

which measures the edges of the parametrised octahedra. The solution set S of regular octahedra on Γ is $S := t^{-1}(0) \cap X$. The subset of S of positively oriented octahedra gives us a well-defined element in the equivariant normal bordism group (see [3])

$$\Omega_1^{G_{or}}(X, const, X \times Y - TX) = \Omega_1(X/_G, const, X \times_G Y - T(X/_G)),$$

since isotopies of Γ change S only by a normal bordism. This element can be shown to be zero [6], which I call a topological counter-example. In particular, the test map t can be deformed G-equivariantly rel $\partial X = (S^2)^6 \setminus X$ to a map t', such that $t'^{-1}(0) \cap X = \emptyset$.

References

[1] H. B. Griffiths, *The topology of square pegs in round holes*, Proc. London Math. Soc. **62** (1991), 647–672.

[2] H. Guggenheimer, *Finite sets on curves and surfaces*, Israel J. Math. **3** (1965), 104–112.

[3] U. Koschorke: *Vector Fields and Other Vector Bundle Morphisms – A Singularity Approach*, Lecture Notes in Mathematics, Vol. 847, Springer-Verlag, 1981.

[4] V. V. Makeev, *Quadrangles inscribed in a closed curve and the vertices of a curve*, J. Math. Sci., Vol 131, No. 1 (2005), 5395–5400.

[5] B. Matschke, *Equivariant Topology and Applications*, diploma thesis, TU Berlin, 2008.

[6] B. Matschke, in preparation.

[7] L. G. Shnirel'man, *On some geometric properties of closed curves* (in Russian), Usp. Mat. Nauk **10** (1944), 34–44.

[8] W. Stromquist, *Inscribed squares and square-like quadrilaterals in closed curves*, Mathematika **36** (1989), 187–197.

[9] O. Toeplitz, *Ueber einige Aufgaben der Analysis situs*, Verhandlungen der Schweizerischen Naturforschenden Gesellschaft in Solothurn **4** (1911), p. 197.

[10] S. T. Vrećica, Živaljević, *Fulton-MacPherson compactification, cyclohedra, and the polygonal pegs problem*, arXiv:0810.1439, 2008.

Optimizing circle arrangements: questions and comments

Robert Connelly

Consider a Boolean expression for an arrangement of overlapping circles in the plane. A simple example is $(B_1 \cup B_2) \cap B_3$, where each B_i is a circular disk with a fixed radius. A sample problem asks when is the area of $(B_1 \cup B_2) \cap B_3$ maximized. When the two disks B_1 and B_2 can be packed inside B_3 any such packing achieves the maximum area. When one of the two disks B_1 or B_2 has a larger radius than B_3, it can cover B_3, and the area of B_3 is the maximum area of the Boolean expression. For the intermediate case, a configuration such as the one in the figure will achieve the maximum area.

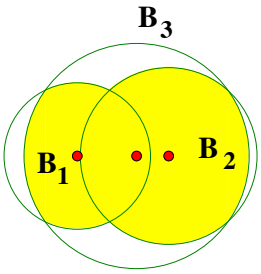

Similarly for the expression $(B_1 \cup B_2 \cdots \cup B_n) \cap B_{n+1}$ when the first disks cannot be packed into or cover the last disk B_{n+1}, there will be some particular optimum configuration. But what can be said about such configurations?

In general it seems that it is quite complicated to determine exact solutions to this type of maximum problem. It is possible, though, to make some observations and to get more information about particular cases. For example, a result of B. Csikós in [2] together with connections to tensegrity structures gives a criterion for the area function to be critical in the space of configurations of disks with fixed radii. This criterion can also be used to verify when a circle with a fixed radius maximizes its intersection with a fixed acute triangle. See the result of B. M. Stewart in [5]. This is also related to the problem of "How must n equal circles (spherical caps) of given angular radius r be arranged on the surface of a sphere so that the area covered by the circles will be as large as possible," which is discussed in the paper [4] by P. W. Fowler and T. Tarnai. Another example is the problem discussed by G. Fejes Tóth in [3]. He shows that "the density of the part of the plane covered by a system of congruent circles of density d is at most $df(1/d)$, where the function $f(x)$ is defined as the maximum of the area of the intersection of a circle of unit area and a hexagon of area x."

The critical formula in [2] can be used in applications to protein folding, where, instead of using energy functions, one can maximize various weighted lattice polynomials of Boolean area/volumes functions of disks. This follows an idea with K. Bezdek in [1]. This has the potential of taking into account not only the pairwise interactions of the atoms, but also their hydrophobic-hydrophilic nature. In addition, using Csikós's theory, the Voronoi construction in [2] should allow a computationally feasible algorithm to compute the gradient of the Boolean area/volume.

References

[1] Károly Bezdek and Robert Connelly, On the weighted Kneser-Poulsen conjecture, (submitted).

[2] Balázs Csikós, On the volume of flowers in space forms. *Geom. Dedicata* 86 (2001), no. 1-3, 59–79.

[3] Gábor Fejes Tóth, Best partial covering of a convex domain by congruent circles of a given total area. *Discrete Comput. Geom.* 38 (2007), no. 2, 259–271.

[4] Patrick W. Fowler and Tibor Tarnai, Transition from spherical circle packing to covering: geometrical analogues of chemical isomerization. *Proc. Roy. Soc. London Ser. A* 452 (1996), no. 1952, 2043–2064.

[5] B. M. Stewart, The two-area covering problem. *Amer. Math. Monthly* 58, (1951). 394–403.

Unfolding convex polyhedra via quasigeodesic source & star unfoldings

Joseph O'Rourke

(joint work with Jin-ichi Itoh and Costin Vîlcu)

1. Introduction

There were two general methods known to unfold the surface $\mathcal{P}$ of any convex polyhedron to a simple polygon in the plane: the source unfolding and the star unfolding. Both unfoldings are with respect to a point $x \in \mathcal{P}$. The source unfolding cuts the cut locus of x on $\mathcal{P}$, and the star unfolding cuts the shortest paths from x to every vertex of $\mathcal{P}$. Our extension replaces x by a simple closed polygonal curve Q. Although we do not yet know the widest classes of curves for which the unfoldings avoid overlap, in both cases the classes include quasigeodesic loops. Again the source unfolding cuts (a portion of) the cut locus, and the star unfolding cuts shortest paths from vertices to Q. And both cut all but a segment of Q.

Quasigeodesics extend the notion of geodesics to nondifferentiable, and in particular, to polyhedral surfaces. Let Γ be any directed curve on a convex surface $\mathcal{P}$, and $p \in \Gamma$ be any point in the relative interior of Γ. Let $L(p)$ be the total face angle incident to the left side of p, and $R(p)$ the angle to the right side. If Γ is a geodesic, then $L(p)=R(p) = \pi$. A *quasigeodesic* Γ loosens this condition to $L(p) \le \pi$ and $R(p) \le \pi$, again for all p interior to Γ [2, p. 16]. A *simple, closed quasigeodesic* is a simple closed curve on $\mathcal{P}$ that is quasigeodesic throughout its length. As all curves we consider must be simple, we will henceforth drop that prefix. Although Pogorelov showed that any convex polyhedron $\mathcal{P}$ has at least three closed quasigeodesics, there is no polynomial-time algorithm known to find them, so we consider instead a wider class. A *geodesic loop* is a closed geodesic with one exceptional *loop point* x at which the condition $L(x)=R(x) = \pi$ may be violated.

2. Quasigeodesic Star Unfolding

$\mathcal{P} \setminus Q$ separates $\mathcal{P}$ into two "halves" P_1 and P_2. If we view the star unfolding as an algorithm, it consists of three main steps:

(1) Select shortest paths $\mathrm{sp}(v_i)$ from each $v_i \in P_k$ to Q.
(2) Cut along $\mathrm{sp}(v_i)$ and flatten each half.
(3) Cut along Q, joining the two halves at an uncut segment $s \subset Q$.

After cutting along $\mathrm{sp}(v_i)$, we conceptually insert an isosceles triangle with apex angle equal to the curvature $\omega(v_i)$ at each v_i, which flattens each half, a technique used by Alexandrov [1]. The procedure is illustrated in Figure 1, and fully described in [3].

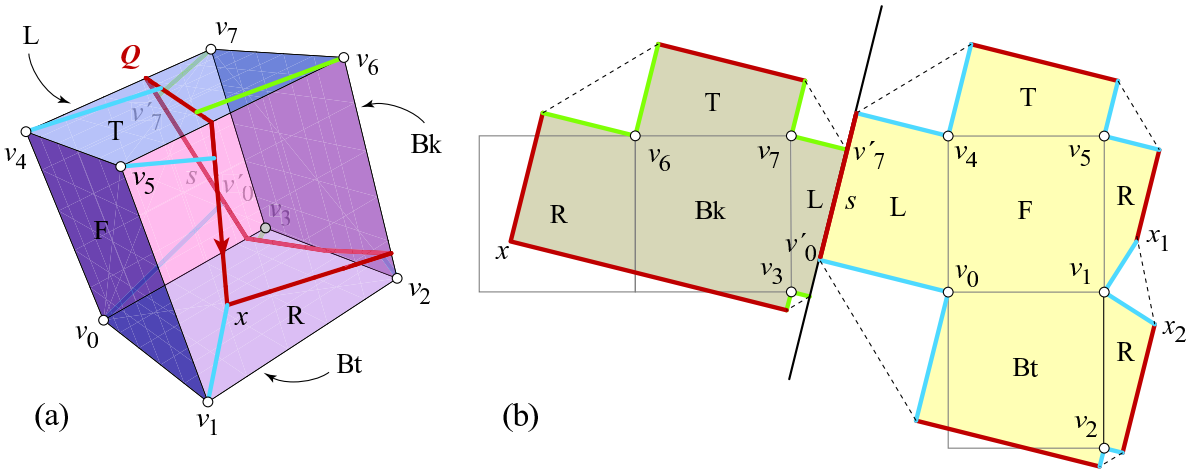

FIGURE 1. (a) Geodesic loop Q on cube. Shortest paths $\mathrm{sp}(v_i)$ are shown. Faces are labeled $\{F, T, L, R, Bt, Bk\}$. (b) Star unfolding with respect to Q, joined at $s = v'_0 v'_7$.

3. Quasigeodesic Source Unfolding

The *point source unfolding* cuts the *cut locus* of the point x: the closure of set of all those points y to which there is more than one shortest path on $\mathcal{P}$ from x. Our method also relies on the cut locus, but now the cut locus C_{P_k} on the half-surface P_k with respect to its boundary $\partial P{=}Q$. We cut only the edges of C_P not incident to Q, plus one further cut. An example of the cut loci for a simple closed quasigeodesic Q are shown in Figure 2.

The main steps of the source unfolding argument for closed quasigeodesics are as follows:

(1) Develop Q to the plane. It is known that a *closed convex curve* develops without self-intersection [4]. Closed quasigeodesics are convex curves to both sides, and quasigeodesic loops are convex to one side.
(2) From a neighborhood of Q in P_k, determine a doubly covered planar cone P_k^* whose boundary is Q. This cone in some sense envelops P_k.
(3) Show that the "peels" of the cut locus of P_k nest inside the peels of the cut locus of P_k^*. This implies that those peels will develop in the plane without overlap by opening P_k^* along a generator of the cone.
(4) The nested embedding is achieved by cutting the cut loci C_{P_1} and C_{P_2} not incident to Q.

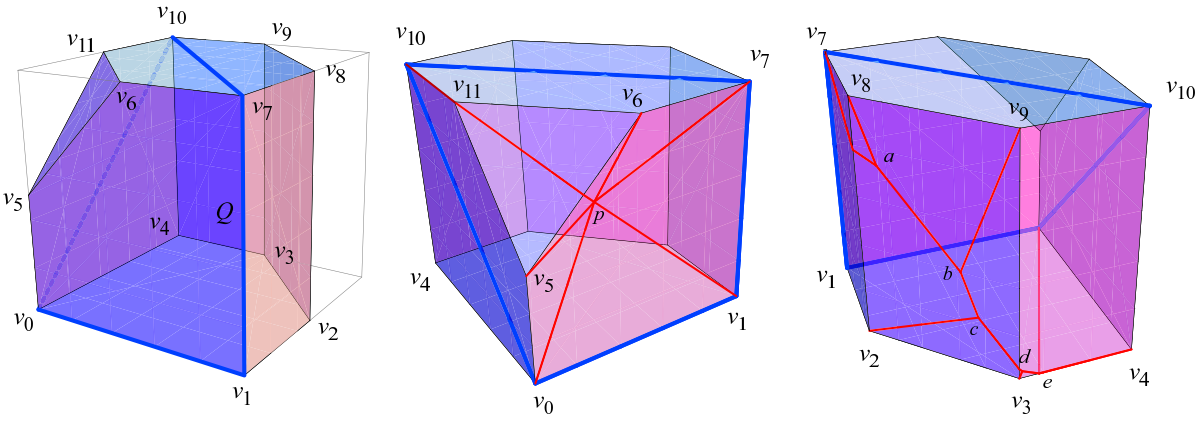

FIGURE 2. (a) Truncated cube and quasigeodesic $Q = (v_0, v_1, v_7, v_{10})$. (b) View of C_{P_1} from "front" side P_1 (c) View of C_{P_2} from "back" side P_2.

(5) Finally, we cut along Q, joining the two halves at an uncut segment $s \subset Q$.

To capture quasigeodesic loops, and in fact all convex curves, the final step above is altered.

Theorem. *Both the source and the star unfolding of a convex polyhedron $\mathcal{P}$ with respect to a quasigeodesic loop Q unfold $\mathcal{P}$ to a simple planar polygon.*

References

[1] Aleksandr D. Alexandrov. *Intrinsic Geometry of Convex Surfaces*. Chapman & Hall/CRC, Boca Raton, FL, 2006. A. D. Alexandrov Selected Works. Edited by S. S. Kutateladze. Translated from the Russian by S. Vakhrameyev.

[2] Aleksandr D. Alexandrov and Victor A. Zalgaller. *Intrinsic Geometry of Surfaces*. American Mathematical Society, Providence, RI, 1967.

[3] Jin-ichi Itoh, Joseph O'Rourke, and Costin Vîlcu. Unfolding convex polyhedra via quasigeodesic star unfoldings. Technical Report 091, Smith College, December 2008. arXiv:0821.2257v1 [cs.CG].

[4] Joseph O'Rourke and Catherine Schevon. On the development of closed convex curves on 3-polytopes. *J. Geom.*, 13:152–157, 1989.

Geometric aspects of discrete elastic rods

Max Wardetzky

(joint work with M. Bergou, S. Robinson, B. Audoly and E. Grinspun)

What this is about

Elastic rods are curve-like elastic bodies that have one dimension (length) much larger than the others (cross-section). Their elastic energy breaks down into three contributions: stretching, bending, and twisting. Stretching and bending are captured by the deformation of a space curve called the *centerline*, while twisting is captured by the rotation of a *material frame* associated to each point on the

centerline. Building on the notions of framed curves, parallel transport, and holonomy, we present a smooth and a corresponding discrete theory that establishes an efficient model for simulating thin flexible rods with arbitrary cross section and undeformed configuration. To large parts, the material herein is an excerpt from [1].

Elastic energy

We describe the configuration of a smooth elastic rod by an *adapted framed curve* $\Gamma = \{\boldsymbol{\gamma}; \mathbf{t}, \mathbf{m_1}, \mathbf{m_2}\}$. Here $\boldsymbol{\gamma}(s)$ is an arc length parameterized space curve describing the rod's *centerline*; the assignment of an orthonormal material frame $\{\mathbf{t}(s), \mathbf{m_1}(s), \mathbf{m_2}(s)\}$ to each point on the centerline contains the requisite information for measuring twist. We require the material frame to be *adapted* to the centerline, *i.e.*, to satisfy $\mathbf{t}(s) = \boldsymbol{\gamma}'(s)$. As usual, we refer to $\boldsymbol{\kappa} = \mathbf{t}'$ as the centerline's *curvature (normal) vector* and to $\tau = \mathbf{m_1'} \cdot \mathbf{m_2}$ as the material frames *twist* measuring the rotation of the material around its centerline. The Kirchhoff model of elastic energy of *inextensible* (no stretching of the centerline) and *isotropic* (no preferred bending direction) elastic rods is given by

$$E = \frac{1}{2} \int_\gamma \alpha \boldsymbol{\kappa}^2 + \beta \tau^2 \, ds \ , \tag{1}$$

where α and β are constants encoding bending and twisting stiffness, respectively.

Curve-angle representation & the Bishop frame

While (1) completely describes an energy model for inextensible isotropic rods, there is a more convenient description when turning to simulations—one that renders the formulation of the material frame more *explicit*. The requisite tool is provided by the *Bishop* (or parallel) frame, an adapted orthonormal frame $\{\mathbf{t}(s), \mathbf{u}(s), \mathbf{v}(s)\}$ that has zero twist uniformly, *i.e.*, $\mathbf{u}' \cdot \mathbf{v} = -\mathbf{v}' \cdot \mathbf{u} = 0$. The assignment of an adapted frame to one point on the curve uniquely pins down the Bishop frame throughout the entire curve. Every smoothly parameterized space curve with nowhere vanishing derivative carries a Bishop frame—one of several properties that sets the Bishop frame apart from the Frenet frame (which is *not* twist-free).

Denoting by θ the angle between the Bishop and the material frame in the cross section orthogonal to the centerline's tangent, *i.e.*, $\theta = \angle(\mathbf{u}, \mathbf{m_1}) = \angle(\mathbf{v}, \mathbf{m_2})$, one readily checks that the material frame's twist satisfies $\tau = \theta'$. Therefore, we can rewrite elastic energy of inextensible isotropic rods as

$$E = \frac{1}{2} \int_\gamma \alpha \boldsymbol{\kappa}^2 + \beta (\theta')^2 \, ds \ .$$

We refer to this formulation as the *curve-angle representation*, as it previously also appeared in [3]. This representation reveals a fascinating analogy between the potential energy of elastic rods and the *kinetic* energy of Lagrange spinning tops. Indeed, by identifying the axis of the top with the direction of the rod's unit tangent, $\mathbf{t}$, and furthermore identifying the rod's arc length with the top's physical

time, we find that $\int \boldsymbol{\kappa}^2 = \int (\mathbf{t}')^2$ and $\int \tau^2 = \int (\theta')^2$ measure the kinetic energy of the motion of the top's center of mass and rotation around its axis, respectively.

Holonomy & Fuller's formula

For a frame to be *parallel* along a space curve has the following interpretation. Consider the centerline's *Gauss image*, $\tilde{\boldsymbol{\gamma}}$, traced out on the unit 2-sphere, $\mathbb{S}^2$, by the unit tangent, $\mathbf{t}$. For $\{\mathbf{u}, \mathbf{v}\}$ to be parallel (twist-free) along $\boldsymbol{\gamma}$ is then equivalent for $\{\mathbf{u}, \mathbf{v}\}$ to be parallel-transported along $\tilde{\boldsymbol{\gamma}}$ in the usual sense of the Levi-Civita connection on $\mathbb{S}^2$.

Assume $\boldsymbol{\gamma}$ is a closed curve, then $\tilde{\boldsymbol{\gamma}}$ is closed as well. When parallel transporting $\{\mathbf{u}, \mathbf{v}\}$ once around $\boldsymbol{\gamma}$ (or $\tilde{\boldsymbol{\gamma}}$), the resulting final frame will usually differ from the initial one by an angle called *holonomy*, *Hol*. This angle is related to the so-called *writhe*. More precisely, whenever $\boldsymbol{\gamma}$ is a non self-intersecting closed space curve with (material) frame $\{\mathbf{m_1}, \mathbf{m_2}\}$, let *Lk* denote the (unique) *linking number* of the two curves $\{\boldsymbol{\gamma}_\pm(s)\} = \{\boldsymbol{\gamma}(s) \pm \epsilon \mathbf{m_1}(s)\}$ for some small enough $\epsilon > 0$. Then

$$Lk = Tw + Wr \ , \tag{2}$$

where $Tw = (1/2\pi) \int_\gamma \tau ds$ is the total *twist* of the material frame, while *writhe* satisfies $Wr \equiv Hol/2\pi$ modulo 1. Equation (2) is sometimes referred to as the Călugăreanu-White-Fuller formula, see, *e.g.*, [2].

Furthermore, the Gauss-Bonnet theorem implies that $Hol \equiv A$ modulo 2π, where A is the signed area enclosed by $\tilde{\boldsymbol{\gamma}}$ on $\mathbb{S}^2$.

Centerline variation

In physical simulations, in order to compute forces, we are required to express changes of elastic energy due to variations of the position (shape) of the centerline. The corresponding change of bending energy, $\int_\gamma \boldsymbol{\kappa}^2 ds$, is straightforward to calculate, while computing the change of twisting energy, $\int_\gamma \tau^2 ds$, is slightly more involved since it requires the computation of the change of holonomy (or writhe). If $\boldsymbol{\gamma}$ is a closed curve, then it follows from Gauss-Bonnet that the change in holonomy, δHol, with respect to varying the centerline's *tangent* (the position of $\tilde{\boldsymbol{\gamma}}$ on $\mathbb{S}^2$) by $\delta\mathbf{t}$ is given by

$$\delta Hol = \delta A = -\int_\gamma \delta\mathbf{t} \cdot (\mathbf{t} \times \mathbf{t}')\, ds \quad \text{and hence} \quad \delta\theta' = \delta\mathbf{t} \cdot (\kappa\mathbf{b}) \ , \tag{3}$$

where $\kappa\mathbf{b} = \mathbf{t} \times \mathbf{t}'$ is the centerline's curvature binormal vector. For closed cuves, (3) is the infinitesimal version of Fuller's calculation for the difference between the writhe of two space curves, see [2]. From (3) we obtain that the L^2-gradient of *Hol* with respect to variations of positions (not tangents) is $(\kappa\mathbf{b})'$.

The discrete picture

We represent a discrete rod's centerline as a piecewise straight polygonal space curve, and we associate discrete adapted orthonormal frames with *edges* of this curve. Along each edge we assume these frames to be constant. For each pair

$(\mathbf{e}_{i-1}, \mathbf{e}_i)$ of consecutive edges, *discrete parallel transport* from one edge to the next is given by rotating by the angle $\angle(\mathbf{e}_{i-1}, \mathbf{e}_i)$ about the normal to the plane spanned by $\mathbf{e}_{i-1}$ and $\mathbf{e}_i$. This gives rise to discrete Bishop (parallel) frames. Accordingly, we obtain a discrete notion of holonomy (or writhe) for closed polygonal curves.

We require elastic energy and hence a discrete notion of curvature and twist. As in the smooth case, twist is nothing but the change of the angle between the Bishop and the material frame at each edge of the polygonal curve, $\boldsymbol{\gamma}$.

Consider once more the Gauss image, $\tilde{\boldsymbol{\gamma}}$ of $\boldsymbol{\gamma}$, on $\mathbb{S}^2$. The vertices of $\tilde{\boldsymbol{\gamma}}$ correspond to unit tangents, $\mathbf{t}_i$, along the edges of $\boldsymbol{\gamma}$, while the edges of $\tilde{\boldsymbol{\gamma}}$ are arcs of great circles. As in the smooth case before, Gauss-Bonnet tells us that discrete holonomy is related to the signed area enclosed by $\tilde{\boldsymbol{\gamma}}$. To obtain forces, it therefore suffices to study variations of this area with respect to variations of the vertices of $\tilde{\boldsymbol{\gamma}}$. To this end, consider an arc of a great circle of length $\phi_i = \angle(\mathbf{t}_{i-1}, \mathbf{t}_i) < \pi$ between $\mathbf{t}_{i-1}$ and $\mathbf{t}_i$ and consider respective variations by $\delta\mathbf{t}_{i-1}$ and $\delta\mathbf{t}_i$ on $\mathbb{S}^2$. Consider further the area swept out by the geodesics that connect the two varying endpoints. It follows (for example by considering Jacobi fields) that this area (and therefore discrete holonomy) satisfies

$$\delta Hol = \delta A = -\frac{\delta\mathbf{t}_{i-1} + \delta\mathbf{t}_i}{2} \cdot (2\tan\frac{\phi_i}{2}\mathbf{b}_i) \quad \text{with} \quad \mathbf{b}_i = \frac{\mathbf{t}_{i-1} \times \mathbf{t}_i}{|\mathbf{t}_{i-1} \times \mathbf{t}_i|},$$

which is the discrete analogue of (3). By *postulating* in the discrete case relation (3) between the gradient of holonomy and curvature, we may define discrete curvatures at the vertices of $\boldsymbol{\gamma}$ by $\kappa_i = 2\tan(\phi_i/2)$, where ϕ_i is the angle between the edges incident to a particular vertex.

For additional material, including anisotropic rods and simulation results, see [1].

References

[1] M. Bergou, M. Wardetzky, S. Robinson, B. Audoly, and E. Grinspun. Discrete elastic rods. In *ACM Transactions on Graphics*, 27(3), 2008. [Proceedings of ACM SIGGRAPH '08]

[2] F. B. Fuller. Decomposition of the linking number of a closed ribbon: A problem from molecular biology. *PNAS*, 75(8):3557–3561, 1978.

[3] J. Langer and D. A. Singer. Lagrangian Aspects of the Kirchhoff Elastic Rod. *SIAM Review*, 38(4):605–618, 1996.

Complex barycentric coordinates for shape deformation

Mirela Ben-Chen

(joint work with Ofir Weber, Craig Gotsman)

Barycentric coordinates are a very useful mathematical tool for computer graphics applications. Since they allow inferring continuous data over a domain from discrete or continuous values on the boundary of the domain, barycentric coordinates are used in a wide range of applications.

Traditionally, barycentric coordinates in $\mathbb{R}^n$ are defined as the real coefficients of an affine combination of vectors in $\mathbb{R}^n$, see for example [FHK06, Flo03]. As such, they operate identically on each coordinate. When working in the plane,

barycentric coordinates in $\mathbb{R}^n$ can also be considered as an affine combination of *complex* numbers with real coefficients, thus it is natural to consider also the case where the coefficients are themselves allowed to be complex. This new point of view has a few advantages: First, it allows the definition of *complex barycentric coordinates*, permitting a *different* linear operation for each of the two coordinates, through which new effects can be achieved. Second, it unleashes the rich theory of complex analysis, simplifying the underlying theory considerably.

Complex barycentric coordinates are especially useful for 2D shape and image deformation. In a typical application scenario, the user defines a *source* contour, usually a polygon, and deforms it to a target contour by moving its vertices. This indicates to the application that the region within the source contour should be deformed in some natural way to the region within the target contour such that the per-edge correspondence is respected. For such applications it is important that the mapping has certain properties - for example, if the target polygon is identical to the source polygon, then the mapping should be the identity map. In addition, for shape deformation applications, conformal mappings are preferred, since they preserve angles and hence preserve details better than arbitrary mappings.

Complex barycentric coordinates are defined as follows. Let $S = \{v_1, v_2, \ldots, v_n\} \subset \mathbb{R}^2$ be the vertices of a simply connected planar polygon, oriented in the counter clockwise direction, $v_j = (x_j, y_j)$. Let $z_j = x_j + iy_j$ be the representation of the vertices as complex numbers, $z_j \in \mathbb{C}$. Denote by Ω the interior of S. Given a point $v = (x, y) \in \Omega$, define $z = x + iy$ and consider the following *complex* linear combination $\sum_{j=1}^{n} k_j(z) z_j$, where $k_j : \Omega \to \mathbb{C}$. We say that the functions $k_j(z)$ are *complex barycentric coordinates* with respect to S if the following two properties hold for all $z \in \Omega$:

$$\textit{Constant precision: } \sum_{j=1}^{n} k_j(z) = 1, \qquad \textit{Linear precision: } \sum_{j=1}^{n} k_j(z) z_j = z$$

Given complex barycentric coordinates $k_j(z)$ for S, we may consider the complex function $g_{S,F}(z)$ which results from applying the complex barycentric coordinates to the vertices of a target polygon $F = \{f_1, f_2, \ldots, f_n\} \subset \mathbb{C}$:

$$g_{S,F}(z) = \sum_{j=1}^{n} k_j(z) f_j$$

Complex barycentric coordinates can easily be generalized to continuous contours in the following way. Let Ω be a simply connected open planar region with a smooth boundary S. Given $z \in \Omega$ and $w \in S$, consider the complex function $k(w, z) : S \times \Omega \to \mathbb{C}$. As in the discrete case, we say that $k(w, z)$ is a barycentric coordinate function if it satisfies the following properties for all $z \in \Omega$:

$$\textit{Constant precision: } \int_S k(w, z)\, dw = 1, \quad \textit{Linear precision: } \int_S k(w, z) w\, dw = z$$

The function $k(w, z)$ is sometimes called a *kernel function*. The integral over S is a *complex* integral, where $dw = T(w)ds$, $T(w)$ is the unit-length tangent vector

to S at w, and ds is the usual arc-length differential element. Given a continuous complex function $f : S \to \mathbb{C}$, we can define a planar mapping $g_{S,f}(\Omega)$ as follows:

$$g_{S,f}(z) = \int_S k(w,z) f(w)\, dw$$

As in the case of real barycentric coordinates, the main challenge is to find kernels $k(w,z)$, or, in the discrete case, coordinate functions $k_j(z)$, which satisfy the required properties. As it turns out, simply choosing the Cauchy kernel $C(w,z) = \frac{1}{2\pi i}\frac{1}{w-z}$ provides us with the required properties. Due to the Cauchy integral formula, we have that for $z \in \Omega$

$$\frac{1}{2\pi i}\int_S \frac{1}{w-z}\, dw = 1, \qquad \frac{1}{2\pi i}\int_S \frac{w}{w-z}\, dw = z,$$

which are the two properties we have required - constant precision and linear precision. We call the resulting coordinates *Cauchy coordinates*.

Applying the Cauchy coordinates to a target contour $f(S)$ defines the following mapping:

$$g_{S,f}(z) = \frac{1}{2\pi i}\int_S \frac{f(w)}{w-z}\, dw$$

This mapping is called the *Cauchy transform* of f [Bel92]. It has various interesting properties, one of which being that if f is continuous on S, then g is always holomorphic on Ω. Hence, if we apply these coordinates in the context of planar shape deformation, the deformation is guaranteed to be conformal (if the derivatives do not vanish). In addition, since holomorphic functions are infinitely differentiable, the mapping will be smooth.

In a practical shape deformation scenario, the contour S is usually a polygon (sometimes called "cage") which the user deforms to a new polygon F with vertices $\{f_1, f_2, \ldots, f_n\}$. By integrating over the edges of the source polygon and taking into consideration that the target contour is also a polygon, we get:

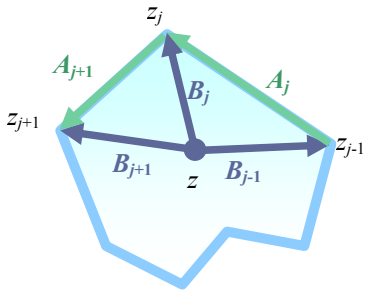

$$g_{S,f}(z) = \sum_{j=1}^{n} C_j(z) f_j$$

$$C_j(z) = \frac{1}{2\pi i}\left(\frac{B_{j+1}(z)}{A_{j+1}}\log\left(\frac{B_{j+1}(z)}{B_j(z)}\right) - \frac{B_{j-1}(z)}{A_j}\log\left(\frac{B_j(z)}{B_{j-1}(z)}\right)\right)$$

As it turns out, these complex coordinates are equivalent to the recently introduced Green coordinates [LLCO08] which generalized the concept of barycentric coordinates to be a linear combination of the coordinates of the vertices of the polygon *plus a linear combination of the normals to the edges of the polygon.*

In addition to the Cauchy-Green barycentric coordinates, we showed how to define coordinates which minimize a given energy functional. We proposed two such functionals, one which improves the fit between the target polygon and the boundary of the resulting deformation (inspired by the continuous Szegö transform), and

one which allows the user to manipulate a small set of positional constraints, instead of manipulating the vertices of the target polygon.

To conclude, we have generalized the concept of barycentric coordinates from real numbers to complex numbers, and provided a few examples of known and new coordinates which can be expressed quite simply in this framework. We believe there is still much research to be done on the theory and applications of complex barycentric coordinates. One challenge is to find non-conformal complex coordinates which will generate the more useful "as rigid as possible"-type deformations. Another interesting theoretical issue is the connection between complex barycentric coordinates and the so-called "primal/dual ratio". As Mercat [Mer08] pointed out, complex primal/dual ratios will arise when the primal and dual edges are not orthogonal. We believe more insight into complex barycentric coordinates can be gained by studying these concepts.

References

[Bel92] Bell S.-R.: *The Cauchy Transform, Potential Theory and Conformal Mapping.* CRC Press, 1992.

[FHK06] Floater M. S., Hormann K., Kòs G.: A general construction of barycentric coordinates over convex polygons. *Adv. Comp. Math.* 24, 1–4 (2006), 311–331.

[Flo03] Floater M. S.: Mean-value coordinates. *Comp. Aided Geom. Design* 20, 1 (2003), 19–27.

[LLCO08] Lipman Y., Levin D., Cohen-Or D.: Green coordinates. *ACM Trans. Graph.* 27, 3 (2008). [Proceedings of ACM SIGGRAPH '08]

[Mer08] Mercat C.: Discrete complex structure on surfel surfaces. *Discrete Geometry for Computer Imagery*, LNCS 4992 (2008), 153–164.

Circle packing sampler

Ken Stephenson

After a brief overview of "circle packing", we discuss three topics of current interest: (1) The "spontaneous geometry" circle packings bring with random triangulations, (2) the "fast geometry" available with a new circle packing algorithm, and (3) the "warped geometry" one sees in affine circle packings.

Circle packings are configurations P of circles having prescribed patterns K of tangency. K can be essentially any triangulation of a topological surface, and the heart of the topic is that P imposes a geometry on K — a geometry that is "conformal" in nature. For general backgound, see [1].

(1) Random Geometry: Circle packing got its start (in analysis) with a conjecture of Thurston regarding the approximation of classical conformal maps by discrete conformal maps — maps between circle packings sharing the same combinatoric pattern K. In the adjustment of circle sizes from one packing to another, conformal structure is (roughly) perserved. His conjecture was proven by Rodin and Sullivan, see [3].

However, fairly extensive experiments suggest that much more may be true: conformal structure seems to be an "emergent" property. A circle packing of a

random triangulation of a region Ω imposes a geometry on Ω. As the complexity of such random triangulations grows, the imposed geometries appear to converge in probability to the conformal geometry Ω inherits from the plane. The following figure illustrates estimates of two companions of conformal structure, harmonic measure and extremal length. On the left is the traditional circle packing approach, which starts with a circle packing of Ω, then repacks it for various purposes. On the right is our alternate approach, which differs only in that the initial triangulation of Ω is random.

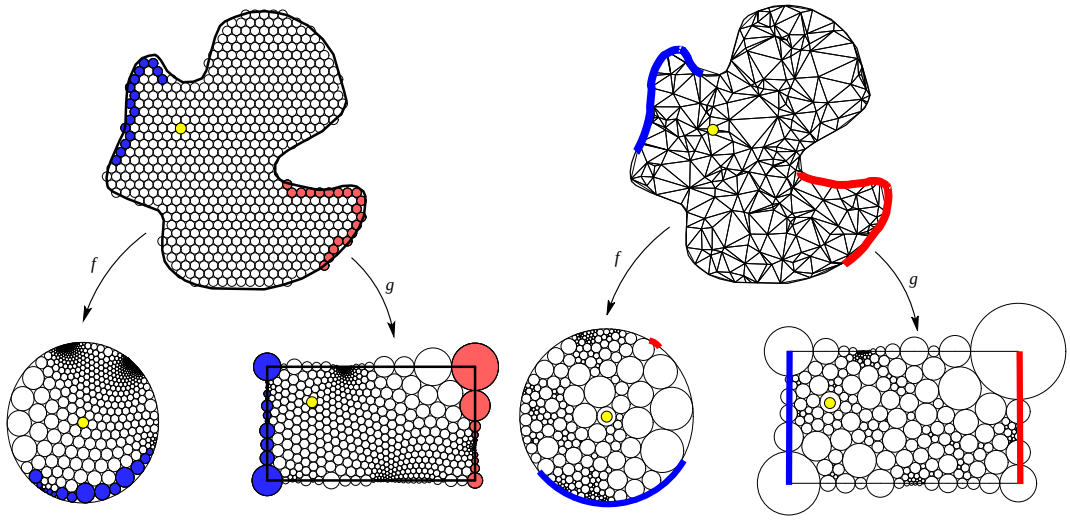

The robustness of convergence of such conformal quantities is suggested by experiments with Ω a square. On the left of the following figure, a random Delaunay triangulation of Ω is packed as a rectangle, with corner circles associated with vertices of K closest to the corners of Ω.

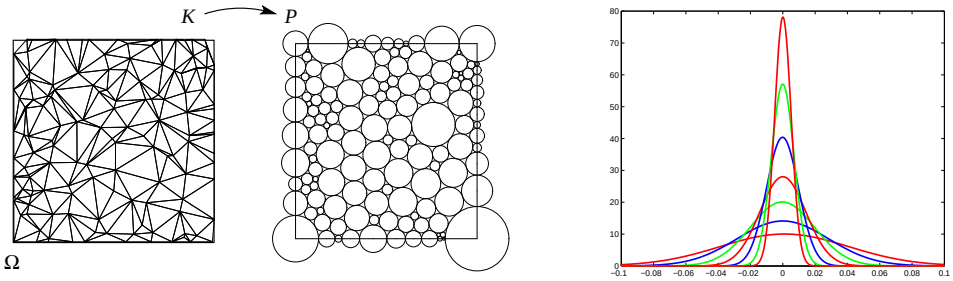

The logarithm of the aspect ratio (width/height) of the resultant rectangle is a random variable which by symmetry will have mean zero. Trial runs are illustrated on the right: each plot gives the distribution of outcomes for 5000 random trials for, respectively, $N = 200, 400, 1600, 3200, 6400$, or 12800 random points in Ω. Observe that doubling the number of points almost precisely halves the variance.

Emergent conformality could have broad implications. By varying the notion of random triangulations, for instance, one might be able to approximate solutions of the Beltrami equation. In applications, there may be a "central limit" theorem justifying circle packing as a mechanism for imposing conformal structures.

(2) Fast Geometry: As combinatorial complexity has grown, circle packing computations have become progressively more unweildy. Current methods compute

local data — radii R — and only then lay out the global configuration, one circle at a time, to get the centers Z. With large packings, even highly accurate radii lead to cumulative layout errors that prevent a coherent global packing. My student, Gerald Orick, has developed a novel new algorithm, applicable now to maximal packings of complexes K triangulating the disc or sphere.

Orick's approach is iterative, but alternates between adjustments to R and to Z via Tutte-style embeddings. Assuming that K triangulates a disc, assign an arbitrary initial radius label R. In each iteration cycle, the current R determines centers for boundary circles as well as geometric weights for a Laplace operator on K. Solving the Dirichlet problem (efficiently done via sparse matrices) gives an embedding of centers Z. The local geometry of the embedding leads to a new label R, and the process repeats. This is extremely fast. For instance, a typical brain flattening application involving 250,000 circles would take half a day on a laptop and might still suffer layout problems. The new algorithm will compute the packing in 3 minutes with no layout problems — in fact, reasonably accurate intermediate layouts will become available within the first few seconds.

The key bit of local geometry is reflected in this image of the star of v: were the embedding associated with a circle packing, all the face sectors at v would have the same radius. When they don't, a new label r is set for v so that $2\pi r^2$ equals the sum of sector areas. Once new labels are set for all vertices, Dubejko-style weights [5] can be computed for the edges, giving a Laplace operator for K. This leads to a new embedding, etc., etc.

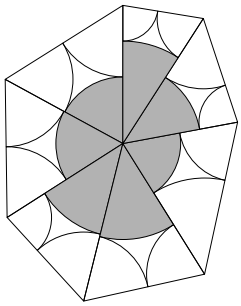

Fast computation can be a game-changer in applications of circle packing.

(3) Warped Geometry: If K triangulates a compact oriented surface, then it imposes, via circle packing, a unique conformal structure on that surface. A new approach to the fundamental packing procedures allows us to compute general "affine" structures. The figure below is based on a combinatorial torus, K. On the left is the associated conformal torus T, determined by laying out a fundamental domain — edge shading indicates side-pairings. On the right is an affine torus for this same K.

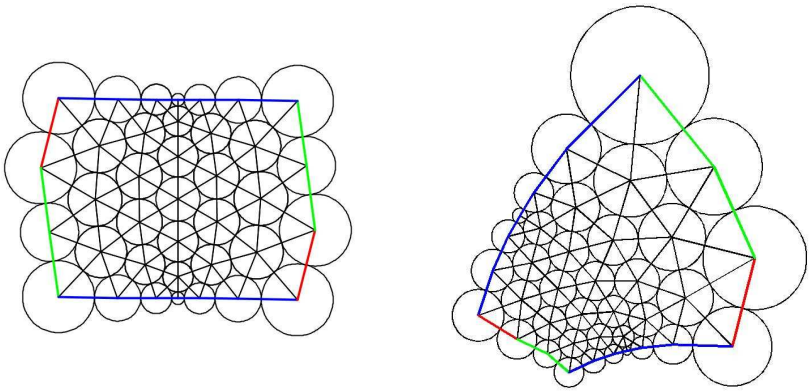

The side-pairing maps for the affine torus are generated by $z \mapsto \alpha z, z \mapsto \beta z$. The construction begins by specifying the moduli $|\alpha|$ and $|\beta|$ and applying a packing

procedure to determine labels $[r_1 : r_2 : r_3]$ (in homogeneous coordinates) for the faces. These induce, for any vertex v, a *locally* consistent set of radii defining a flower for v. In general, however, there is no *globally* consistent set of radii. $\mathrm{Arg}(\alpha)$ and $\mathrm{Arg}(\beta)$ are uniquely determined in the packing process, reflecting the anticipated rigidity associated with K.

Circle "packings" consisting of one self-tangent circle have been used to study the space of affine tori as fibered over the space of conformal tori, [2]. Now one can experiment not only with more general combinatorial tori, but also with higher genus surfaces. These affine structures also suggest an approach to discrete holomorphic differential forms.

References

[1] Ken Stephenson, "Introduction to Circle Packing: The Theory of Discrete Analytic Functions", Camb. Univ. Press 2005, New York.

[2] S. Kojima, S. Mizushima, and S. P. Tan, *Circle packings on surfaces with projective structures*, J. Differential Geom., **63** (2003), 349–397.

[3] B. Rodin and D. Sullivan, *The convergence of circle packings to the Riemann mapping*, J. Differential Geom., **26** (1987), 349–360.

[4] William Thurston, *The finite Riemann mapping theorem*, unpublished talk at An International Symposium at Purdue University in celebrations of de Branges' proof of the Bieberbach conjecture, 1985.

[5] Tomasz Dubejko, *Circle-packing connections with random walks and a finite volume method*, Sémin. Théor. Spectr. Géom., **15** (1996–97), 153–161.

Reporter: Boris Springborn

Participants

Ulrich Bauer
Mathematisches Institut
Georg-August-Universität
Bunsenstr. 3-5
37073 Göttingen

Mirela Ben-Chen
Computer Science Department
TECHNION
Israel Institute of Technology
Haifa 32000
ISRAEL

Bruno Benedetti
Institut für Mathematik
MA 6-2
Technische Universität Berlin
Straße des 17. Juni 136
10623 Berlin

Prof. Dr. Ethan Bloch
Department of Mathematics
Bard College
Annandale-on-Hudson , NY 12504
USA

Prof. Dr. Alexander I. Bobenko
Institut für Mathematik
Fakultät II - Sekr. MA 8 - 3
Technische Universität Berlin
Straße des 17. Juni 136
10623 Berlin

Prof. Dr. Ulrich Brehm
Institut für Geometrie
TU Dresden
01062 Dresden

Dr. Ulrike Bücking
Institut für Mathematik
Fakultät II - Sekr. MA 8 - 3
Technische Universität Berlin
Straße des 17. Juni 136
10623 Berlin

Prof. Dr. Robert Connelly
Department of Mathematics
Cornell University
Malott Hall
Ithaca , NY 14853-4201
USA

Prof. Dr. Herbert Edelsbrunner
Department of Computer Science
Duke University
Box 90129
Durham , NC 27708-0129
USA

Felix Effenberger
Fachbereich Mathematik
Institut für Geometrie u. Topologie
Universität Stuttgart
Pfaffenwaldring 57
70550 Stuttgart

Dipl. Math. Martin von Gagern
Zentrum für Mathematik
TU München
Boltzmannstr. 3
85748 Garching bei München

Dr. Udo Hertrich-Jeromin
Department of Mathematical Sciences
University of Bath
Claverton Down
GB-Bath BA2 7AY

Prof. Dr. Tim Hoffmann
Zentrum für Mathematik
TU München
Boltzmannstr. 3
85748 Garching bei München

Emanuel Huhnen-Venedey
Institut für Mathematik
MA 8 - 3
Technische Universität Berlin
Straße des 17. Juni 136
10623 Berlin

Dr. Ivan Izmestiev
Institut für Mathematik
MA 8 - 3
Technische Universität Berlin
Straße des 17. Juni 136
10623 Berlin

Prof. Dr. Michael Joswig
Fachbereich Mathematik
TU Darmstadt
Schloßgartenstr. 7
64289 Darmstadt

Prof. Dr. Richard Kenyon
Department of Mathematics
Brown University
Box 1917
Providence , RI 02912
USA

Prof. Dr. Wolfgang Kühnel
Fachbereich Mathematik
Institut für Geometrie u. Topologie
Universität Stuttgart
Pfaffenwaldring 57
70550 Stuttgart

Dr. Carsten Lange
Institut für Mathematik
Freie Universität Berlin
Arnimallee 3
14195 Berlin

Inna Lukyanenko
Institut für Mathematik
MA 8 - 3
Technische Universität Berlin
Straße des 17. Juni 136
10623 Berlin

Prof. Dr. Feng Luo
Department of Mathematics
Rutgers University
Hill Center, Busch Campus
110 Frelinghuysen Road
Piscataway , NJ 08854-8019
USA

Dr. Frank H. Lutz
Fakultät II-Institut f. Mathematik
Technische Universität Berlin
Sekr. MA 3-2
Straße des 17. Juni 136
10623 Berlin

Dr. Benjamin Matschke
Fachbereich Mathematik, Sekr.MA 8-5
Technische Universität Berlin
Straße des 17. Juni 136
10623 Berlin

Prof. Dr. Christian Mercat
Departement de Mathematiques
Universite Montpellier II
Place Eugene Bataillon
F-34095 Montpellier Cedex 5

Prof. Dr. Joseph O'Rourke
Department of Computer Science
Smith College
Clark Science Center
Northampton MA 01063
USA

Prof. Dr. Yann Ollivier
35, rue Rene Leynaud
F-69001 Lyon

Prof. Dr. Igor Pak
School of Mathematics
University of Minnesota
127 Vincent Hall
206 Church Street S. E.
Minneapolis MN 55455-0436
USA

Prof. Dr. Gaiane Panina
Institute for Informatics and Automation
RAS
14, lin, V.O.39
199171 St. Petersburg
Russia

Prof. Dr. Ulrich Pinkall
Fakultät II-Institut f. Mathematik
Technische Universität Berlin
Sekr. MA 3-2
Straße des 17. Juni 136
10623 Berlin

Prof. Dr. Konrad Polthier
Institut für Mathematik
Freie Universität Berlin
Arnimallee 3
14195 Berlin

Prof. Dr. Jürgen Richter-Gebert
Zentrum für Mathematik
TU München
Boltzmannstr. 3
85748 Garching bei München

Dr. Günter Rote
Institut für Informatik
Freie Universität Berlin
Takustr. 9
14195 Berlin

Wolfgang K. Schief
Institut für Mathematik
MA 8 - 3
Technische Universität Berlin
Straße des 17. Juni 136
10623 Berlin

Prof. Dr. Jean-Marc Schlenker
Institut de Mathematiques de Toulouse
Universite Paul Sabatier
118, route de Narbonne
F-31062 Toulouse Cedex 9

Michael Schmid
Zentrum für Mathematik
Technische Universität München
Boltzmannstr. 3
85748 Garching bei München

Bernd Schulze
Department of Mathematics
York University
4700 Keele Street
North York , Ont. M3J 1P3
CANADA

Stefan Sechelmann
Institut für Mathematik
Fakultät II - Sekr. MA 8 - 3
Technische Universität Berlin
Straße des 17. Juni 136
10623 Berlin

Dr. Boris Springborn
Institut für Mathematik
Fakultät II - Sekr. MA 8 - 3
Technische Universität Berlin
Straße des 17. Juni 136
10623 Berlin

Prof. Dr. Kenneth Stephenson
Department of Mathematics
University of Tennessee
121 Ayres Hall
Knoxville , TN 37996-1300
USA

Prof. Dr. Ileana Streinu
Department of Computer Science
Smith College
Clark Science Center
Northampton MA 01063
USA

Prof. Dr. John M. Sullivan
Fakultät II-Institut f. Mathematik
Technische Universität Berlin
Sekr. MA 3-2
Straße des 17. Juni 136
10623 Berlin

Prof. Dr. Yuri B. Suris
Zentrum für Mathematik
Technische Universität München
Boltzmannstr. 3
85748 Garching bei München

Prof. Dr. Serge Tabachnikov
Department of Mathematics
Pennsylvania State University
University Park , PA 16802
USA

Prof. Dr. Johannes Wallner
Institut für Geometrie
TU Graz
Kopernikusgasse 24
A-8010 Graz

Prof. Dr. Max Wardetzky
Institut für Numerische
und Angewandte Mathematik
Universität Göttingen
Lotzestr. 16-18
37083 Göttingen

Prof. Dr. Günter M. Ziegler
Institut für Mathematik
MA 6-2
Technische Universität Berlin
Straße des 17. Juni 136
10623 Berlin